AN INVESTIGATION OF BIAS IN SPECTRAL MEASUREMENT OF TURBULENT FLOWS USING THE LASER DOPPLER ANEMOMETER

BY

MICHAEL N. KOTAS

A thesis submitted to the
Faculty of the Graduate School of
the State University of New York at Buffalo
in partial fulfillment of the requirements for the degree of
Master of Science.

January 1989

DEDICATION

Dedicated to Geraldine and Norbert Kotas.

TABLE OF CONTENTS

ACKNOWLEDGEMENTS

I would like to take this opportunity to acknowledge my gratitude to the following people for their help during the course of this work.

Scott Woodward, without whose help I probably would never have finished, Hussein Hussein, for doing alot of dirty work which I never would have done for him, Ole Strange, whom I could never have faced again if I didn't finish, Preben Buchhave, for being hip, Eileen Graber, whom I could never have faced again if I didn't finish, Kay Ward, for her final strokes of shear genius, Andre Soom, for approving things, Jim Tan-At-Achat, for his inspiring dedication to his (and everybody else's) work, Wayne Dussault, for being so obnoxious, Victor Demjenko, for getting the serial interface to work, and also my thesis committee, Dr. B. Lieber, Dr. Dale Taulbee, Dr. Steve Capp, (where were you for the defense, Steve?) also, Aamir Shabir, Stew Leib, Sunil Kumar, Tai Kuan Woo, De Xiu Peng, Jim Sonnenmeir, Bob Suhoke, Jr., Bob Brandt, Stan Kowalski, Paul Kotas, Engin Arik, Jim Hartel, Susanne Johnson, and Philippe Gosez.

I would especially like to thank my advisor, Dr. William K. George, for his inspiration, encouragement, and longsuffering (real long suffering.)

ABSTRACT

An unique spectral estimator is derived from the interpretation of the output of the laser Doppler anemometer (operated under conditions of low seeding density) as an analog signal which is blank much of the time. This estimator is used in a data processing scheme on measurements obtained in a turbulent axi-symmetric free jet to calculate the power spectral density. The results are investigated with respect to the estimator's ability to eliminate bias.

LIST OF FIGURES

Chapter 1: INTRODUCTION

Most laser Doppler anemometer (LDA) measurements are performed under conditions of low seeding density using a signal processor capable of resolving the Doppler frequency of single particles crossing the measurement volume. Examples of this application include virtually all wind tunnel experiments, most measurements in gases, and many liquid flows. By definition, low seeding density means that on the average, less than one particle is in the measurement volume at a time. In other words, it is rare that more than one particle is in the measurement volume and much of the time there are no particles in the measurement volume. This mode of operation is also referred to as "burst mode" or "individual realization mode" of operation of the LDA and is the most common mode of operation of LDA systems. The velocity record obtained with the LDA operated under these conditions is characterized as intermittent and stochastic; velocity measurements are the result of random particle arrivals.

A problem associated with LDA measurements made under conditions of low seeding density is that statistical calculations based on measured particle velocities do not necessarily correspond to the statistical properties of the fluid at the measurement point. This steady and systematic error in the calculation of statistical results is called bias. Bias can be defined as the difference between the average value calculated on the basis of an estimate and the true average value.

More rigorously, assume X(t) is a stationary random process of infinite duration, for which is known only a single sample function X(t), for $0 \le t \le T$. On the basis of this sample function, one wishes to estimate

parameters (i.e.:moments) of the random process itself. However, the estimates are also random since they depend on which particular sample function is used.

Consider an unknown parameter θ, which one wishes to estimate by the random parameter θ_e. The expected value of θ_e can be calculated using the expectation operation, E( ):

$$E\langle\theta_e\rangle = \int_{-\infty}^{\infty} \theta\, p(\theta)\, d\theta \qquad 1.1$$

where $p(\theta)$ is the probability density function of θ.

It is usually desired that the average value of the estimate $E\langle\theta_e\rangle$ would be the quantity to be estimated, θ. When this isn't the case, the difference between these two quantities is said to be the bias in the estimate of θ

$$bias = E\langle\theta_e\rangle - \theta \qquad 1.2$$

For this investigation the bias in power spectral density will be defined as the difference between the averaged biased and unbiased spectral estimates, 2.2.8 and 2.3.1.

$$bias_{LDA} = \overline{S}_T(f)_{biased} - \overline{S}_T(f)_{unbiased} \qquad 1.3$$

This form of bias in LDA measurements is usually referred to as "velocity bias" and is caused by a correlation between the fluid velocity and particle statistics. It should be emphasized that, throughout the text, discussions concerning bias refer to <u>velocity</u> <u>bias</u>,

unless otherwise indicated. This is distinguished from other types of bias, in particular, the statistical bias usually referred to in spectral estimation theory.

The problem of bias can be illustrated by the following example. Suppose an LDA measurement volume is located in a region where seeded and unseeded fluid cross the measurement volume intermittently. This would be the case for instance, at the edge of a free jet where the primary fluid is seeded and the ambient fluid is not. When the unseeded fluid crosses the measurement volume, realizations of velocity diminish or disappear. If the entrained fluid moves slower than the seeded fluid (which will usually be the case in a jet) it is clear that the average velocity measured by the LDA will be wrong. Since the velocity of <u>particles</u> is measured, and the slow moving fluid has fewer or no particles in it, velocity realizations of slow moving <u>fluid</u> are fewer than velocity realizations of rapidly moving <u>fluid</u>. Therefore, the ensemble average of particle velocity will not represent the time average velocity of the fluid at the measurement point.

This example can be generalized and the problem of velocity bias stated as follows: ensemble averaging measured particle velocities will yield incorrect time averages of fluid velocity if there is any correlation between the fluid velocity and the particle statistics. In other words, the sampling process must be independent of the sampled process.

This important problem has long been recognized (cf: McLaughlin and Tiederman 1972), although the technique for correcting it is still a subject of debate. The motivation for resolving this problem rests in its applicability to a wide class of applications: LDA systems operated under conditions of low seeding density in turbulent flows. In these

applications, the particle statistics are correlated with the fluid velocity, for example, more particles cross the measurement volume per unit time at high speeds than at low speeds. When turbulence intensity is high, the effect of velocity bias may be substantial.

George (1976) and Buchhave (1979) have shown that velocity bias can be corrected for in LDA measurements by weighting particle velocity by residence time (the time during which the particle resides in the LDA measurement volume.) This technique, referred to generally as "residence time weighting," is based on a mathematical proof in which the statistical characteristics of particles moving in a Lagrangian reference are related to the statistical characteristics of the fluid in a stationary Eulerian reference (Stevenson 1974.)

The only assumption involved in the residence time analysis is that the particles are statistically uniformly distributed in space. While there may be other assumptions which may insure the statistical independence of the particle arrivals and the velocity, this is the only one which has been discovered to date. All of the models proposed for the burst-mode signal depend on assumptions about how the particle and velocity statistics are related (e.g. Edwards 1981, Adrian and Yao 1987).

The validity of residence time weighting has been verified experimentally in a number of independent investigations (Buchhave 1979, Capp 1983, Hussein 1988.)

An example of the residence time weighting algorithm can be given for illustration purposes. The mean velocity, $\bar{u}$, determined using a simple

ensemble average is biased:

$$\bar{u}_{biased} = \frac{1}{N}\sum_{i=1}^{N} u_i . \qquad 1.4$$

The residence time weighted mean value $\bar{u}$ is unbiased:

$$\bar{u}_{unbiased} = \frac{\sum_{i=1}^{N} u_i \Delta t_i}{\sum_{i=1}^{N} \Delta t_i} \qquad 1.5$$

The subscript "i" refers to the i^{th} particle crossing the beam, u_i is its velocity and Δt_i is its residence time.

An interesting implication of the technique of residence time weighting is that the discontinuous digital signal is interpreted as a continuous analog signal: time averages are calculated using integration during residence times. A spectral analysis algorithm can be derived using a similar interpretation of the discontinuous digital signal.

The impact of the residence time weighting technique on measurements of power spectral density of turbulent flows has received little attention. Only one known previous investigator, Buchhave (1979) has attempted to implement a scheme to correct for bias in measurements of power spectral density using residence time weighting. This investigation is an outgrowth of that work to more completely establish the effects of residence time weighting on measurements of power spectral density.

The strategy which will be adopted in this thesis is to decouple the particle statistics from the fluid velocity by uniformly seeding the environment and treat the discontinuous velocity record as if it were continuous. Using this interpretation, an estimator for power spectral density is derived using residence time weighted Fourier coefficients.

This has been described in detail in George (1988). The power spectral density estimator obtained is used in a data processing scheme on measurements obtained in a turbulent flow and the results are investigated to determine the estimator's ability to eliminate bias.

Two conflicting problems affected the algorithm implemented by Buchhave (1979). On the one hand, a double summation incorporated to calculate the spectral estimate slowed down the processing time prohibitively, while on the other, decreasing the block length used (to compensate for this effect) created oscillations in the measured spectrum (see the discussion in Section 7.3.)

By incorporating a new algorithm ("The Rapid Recursive Spectral Analysis Algorithm"), which replaces the double summation by a single summation (Section 2.2), and implementing a rapid recursive Fourier transform (Section 4.3), both of these difficulties were overcome. The result is a fast calculation scheme which processes long blocks of randomly sampled data quickly, to provide spectral estimates which are free from velocity bias and oscillations.

Chapter 2: DEFINITION OF TERMS

2.1 Power Spectral Density Estimation Based on the Finite Fourier Transform

The power spectral density can be defined as the ordinary Fourier integral transform of the autocorrelation, $R(\tau)$ of a stationary random process, u(t).

$$S(f) = \int_{-\infty}^{\infty} R(\tau) e^{j2\pi ft} d\tau \qquad 2.1.1$$

$$R(\tau) = E\{u(t)u(t+\tau)\} \qquad 2.1.2$$

where E{ } is the expectation operator.

The power spectral density may also be interpreted as the integral of the autocorrelation of the Fourier transform of the random process over all frequencies.

$$S(f) = \int_{-\infty}^{\infty} E\left\{\hat{u}(f')\hat{u}^*(f)\right\} df' \qquad 2.1.3$$

$$\hat{u}(f) = \int_{-\infty}^{\infty} u(t) e^{j2\pi ft} dt \qquad 2.1.4$$

From a single sample function of a random process u(t) it is clear that the Fourier integral transform of u(t) cannot be computed because the data are not known for infinite time. However, the finite Fourier transform

$$\hat{u}_{T_\infty}(f) = \int_0^T u(t) e^{j2\pi ft} dt \qquad 2.1.5$$

can be calculated. Further,

$$E\left\{\hat{u}_{T_\infty}(f)\hat{u}^*_{T_\infty}(f)\right\} = \int_0^T dt \int_0^T R(t-t') e^{j2\pi f(t-t')} dt' \qquad 2.1.6$$

$$E\left\{\hat{u}_{T_-}(f)\hat{u}^{*}_{T_-}(f)\right\} = T\left[\int_{-T}^{T} R(\tau)e^{j2\pi f\tau}d\tau - \frac{1}{T}\int_{-T}^{T}|\tau|R(\tau)e^{j2\pi f\tau}d\tau\right] \quad 2.17$$

where $\tau = t - t'$, and the integral relation,

$$\int_0^T dt\int_0^T dt' F(t-t') = \int_{-T}^{T} F(\tau)(T-|\tau|)d\tau \qquad 2.1.8$$

has been employed. In this equation, $F(\tau)$ is any function of the variable τ.

If u(t) is completely random, the second integral in 2.1.7 is finite. Therefore, it follows from equation 2.1.1 that,

$$\lim_{T\to\infty}\frac{1}{T}E\{\left|\hat{u}_{T_-}(f)\right|^2\} = S(f) \qquad 2.1.9$$

Therefore, the power spectral density may be recovered from the finite Fourier transform of the random process u(t) in the limit as $T\to\infty$.

Based on relation 2.1.9, a class of power spectral density estimates

$$S_T(f) = W_S\left|\hat{u}_T\right|^2 \qquad 2.1.10$$

may be introduced where,

$$\hat{u}_T(f) = \int_{-\infty}^{\infty} d(t)u(t)e^{j2\pi ft}dt \qquad 2.1.11$$

is a Fourier transform of the data as seen through a data window, d(t). The data window has the property that d(t) = 0 for $0 < t > T$, to assure that unavailable data are not required. W_S is a correction factor, to be determined.

The mean value of $S_T(f)$ is given by:

$$E\{S_T(f)\} = W_s \int_{-\infty}^{\infty} dt' \int_{-\infty}^{\infty} dt d(t') d(t) R(t-t') e^{j2\pi f(t-t')} \qquad 2.1.12$$

$$= \int_{-\infty}^{\infty} W_s \int_{-\infty}^{\infty} d(t) d(t-\tau) dt R(\tau) e^{j2\pi f \tau} d\tau \qquad 2.1.13$$

Comparing this expression with the equivalent expression obtained for the mean value of the spectral estimate obtained using the Blackman Tukey technique (equation 2.1.1 with a lag window, $w_T(\tau)$ introduced):

$$E\{S_T(f)\} = \int_{-\infty}^{\infty} w_T(\tau) R(\tau) e^{j2\pi f \tau} d\tau \qquad 2.1.14$$

shows that the two equations are identical as long as,

$$w_T(\tau) = W_s \int_{-\infty}^{\infty} d(t) d(t-\tau) dt \qquad 2.1.15$$

which is a convolution of the data window with itself.
Since a lag window has the power preserving property that $w_T(0) = 1$, the correction factor W_s can be calculated.

$$w_T(0) = W_s \int_{-\infty}^{\infty} d^2(t) dt = 1 \qquad 2.1.16$$

$$W_s = \frac{1}{\int_{-\infty}^{\infty} d^2(t) dt} \qquad 2.1.17$$

Substituting W_s into 2.1.10, yields:

$$S_T(f) = \frac{1}{\int_{-\infty}^{\infty} d^2(t) dt} \left| \int_{-\infty}^{\infty} d(t) u(t) e^{j2\pi f t} dt \right|^2 \qquad 2.1.18$$

This is the complete expression for the power spectral estimate, $S_T(f)$ calculated on the basis of the Fourier transform of the random process

u(t).

2.2 Derivation of Unbiased Estimator

The time record of a component of the velocity, u(t) of a turbulent flow as measured by a laser Doppler anemometer system can be accurately modeled by $u_0(t)$ as indicated in Figure 2.2.1. The variables represented are: velocity component, u_i, particle residence time, Δt_i, and absolute particle arrival time, t_i.

The subscript "i" refers to the i^{th} particle crossing the measurement volume during time T, and i = 1, 2, 3, ... N. "N" is a random variable dependent on the system data rate, and the block averaging time, T. It will be assumed that the particle moves at the same velocity as the fluid and that the fluid velocity does not change appreciably over the measurement volume.

$u_0(t)$ is a discontinuous function which only contributes information about u(t) during the times Δt_i when a particle is in the measurement volume. Inserting $u_0(t)$ into Equation 2.1.18, and assuming d(t) to be a boxcar data window of length, T yields:

$$S_{0T}(f) = \frac{1}{T}\left[\left|\int_0^T u_0(t)e^{j2\pi ft}dt\right|^2\right] \qquad 2.2.1$$

The Fourier transform in the above expression may be approximated as:

$$\hat{u}_{0T}(f) = \sum_{i=1}^{N} u_i \Delta t_i e^{j2\pi ft_i} \qquad 2.2.2$$

where the variation of $\exp(j2\pi ft_i)$ over the interval Δt_i has been neglected.

$\hat{u}_{oT}(f)$ is the discontinuous counterpart of $\hat{u}_T(f)$ with u(t) replaced by $u_o(t)$. including a boxcar window of length T. Inserting equation 2.2.2 into 2.2.1 yields:

$$S_{oT}(f) = \frac{1}{T}\left|\sum_{i=1}^{N} u_i \Delta t_i e^{j2\pi f t_i}\right|^2 \qquad 2.2.3$$

It has been shown, George (1979) that the relationship between the second order expected values $\bar{S}_{oT}$. and $\bar{S}_T$ is:

$$\bar{S}_{oT}(f) = (\mu V)^2 \bar{S}_T(f) \qquad 2.2.4$$

Where μ is the particle number concentration, and V is the measurement volume size. Using the fact that the average particle number concentration in the measurement volume is equal to the fraction of total time particles reside in the volume, $\mu V = \sum_i \Delta t_i / T$, the unbiased spectral estimate can be established in terms of measurable quantities.

$$S_T(f) = \frac{T}{\sum_{i=1}^{N} \Delta t_i}^2 \left|\hat{u}_{oT}(f)\right|^2 \qquad 2.2.5$$

$$S_T(f) = \frac{T}{\left(\sum \Delta t_i\right)^2} \sum_{\substack{i=1 \\ i \neq j}}^{N} \sum_{j=1}^{N} u_i u_j \Delta t_i \Delta t_j e^{j2\pi f(t_i - t_j)} \qquad 2.2.6$$

Rearranging terms yields:

$$S_T(f) = \frac{T}{\sum_i \Delta t_i}^2 \left\{ \sum_{i \neq j} \sum u_i u_j \Delta t_i \Delta t_j e^{j2\pi f(t_i - t_j)} + \sum_i u_i^2 \Delta t_i^2 \right\} \qquad 2.2.7$$

The second term on the right hand side of the above expression represents a false constant shift in the magnitude of the spectral estimate caused by the contribution to the autocorrelation of $u_o(t)$ for

the delay time during which the particle is still in the measurement volume, Buchhave (1979.) Subtracting this term and renormalizing the constant $T/\sum \Delta t_i$ yields:

$$S_T(f) = \frac{T}{\left(\sum \Delta t_i\right)^2 - \sum \Delta t_i^2)} \left\{ \left| \sum_i u_i \Delta t_i d_i e^{j2\pi f t_i} \right|^2 - \sum_i \left(u_i \Delta t_i d_i\right)^2 \right\} \quad 2.2.8$$

Where d_i is the (boxcar) data window. This expression is the unbiased spectral estimate used to calculate the power spectral density, $S_{T_{unbiased}}$ using the technique of block averaging:

$$\overline{S}_T = \frac{1}{M} \sum_{m=1}^{M} S_{Tm} \quad 2.2.9$$

where S_{Tm} is the spectral estimate S_T calculated from the m^{th} block of data.

Note that (except for the renormalized denominator in 2.2.8) Equation 2.2.7 and 2.2.8 are identical, i.e.: they both calculate the unbiased spectral estimate $S_T(f)$. However, an important difference between these two equations is apparent; Equation 2.2.7 incorporates a double summation, whereas 2.2.8 incorporates a single summation. It is clear that the single summation will be computationally faster than the double sum for evaluating $S_T(f)$. A unique aspect of the present work is the incorporation of the single sum expression, rather than the double sum, (as was previously used, Buchhave 1979) to accelerate data reduction.

2.3 Biased and Unbiased Estimators

The spectral estimate derived in Section 2.2 utilizes residence time weighting in the calculation of the Fourier coefficients and has been shown by George (1976) to be unbiased.

An analogous expression has been derived, Thompson (1971) for spectral estimation from randomly sampled data which does not include residence time weighting to correct for velocity bias. This spectral estimate will be referred to as the "biased" estimator.

$$S_T(f)_{biased} = \frac{T}{N^2}\{\left|\sum_i u_i d_i e^{j2\pi f t_i}\right|^2 - \sum_i (u_i d_i)^2\} \qquad 2.3.1$$

Notice the similarity in form to equation 2.2.8. This expression is the biased spectral estimate used to calculate the power spectral density $S_T(f)_{biased}$ using the technique of block averaging.

2.4 FFT Representation of Power Spectral Density

The Fast Fourier Transform provides an alternative method of calculating spectral estimates. The FFT requires equispaced samples taken at intervals which are determined independently from the process being sampled and cannot, therefore, be used directly on randomly spaced LDA data. It can, however, be used to calculate unbiased spectral estimates from analog instruments (i.e.: hot wires,) when used in conjunction with an A/D converter. In terms of the variables previously defined, the spectral estimate calculated by the FFT algorithm is:

$$S_T(f)_{FFT} = \frac{T}{N^2}\{|\sum_i u_i e^{j2\pi f t_i}|^2\}. \qquad 2.4.1$$

This expression is the unbiased spectral estimate used to calculate the power spectral density $S_T(f)_{FFT}$ from the hot wire anemometer output using the technique of block averaging.

2.5 Variance of the Spectral Estimate

The variance of the spectral estimator defined as:

$$var\{S_T(f)\} = E\{S_T^2(f)\} - E^2\{S_T(f)\} \qquad 2.5.1$$

has been derived by Gaster and Roberts (1977) for randomly sampled data, the result shows that as T $\to\infty$,

$$var\,S_T(f)\} \to \left(S(f) + \frac{\sigma^2}{\nu}\right)^2. \qquad 2.5.2$$

Where S is the true power spectral density of u(t), $\nu = N/T$ is the average data rate, and σ is the standard deviation.

$$\sigma^2 = \overline{(u(t) - \bar{u})^2} \qquad 2.5.3$$

By rearranging terms, we can arrive at an expression for the relative error, ϵ.

$$\epsilon^2 = \frac{var\{S_T(f)\}}{S^2(f)} = \left(1 + \frac{\sigma^2}{\nu S(f)}\right)^2 \qquad 2.5.4$$

This expression differs from the equivalent result obtained for continuous signals by the appearance of the second term on the right hand side. Since the spectrum is assumed to drop as frequency increases, the effect of sampling is to increase the relative error of the spectral estimate with frequency. Note also that relative error decreases with increasing average data rate.

The above expression for relative error was derived for the biased spectral estimator 2.3.1 and is only valid in the limit as T $\rightarrow\infty$. The asymptotic unbiased estimate S_T can be shown to have a spectral variance which reduces to the same expression, George (1976), Buchhave (1979.)

Block averaging reduces the relative error of the mean spectral estimate. The governing relation is:

$$\epsilon^2 = \frac{var\{\overline{S}_T(f)\}}{m^2\overline{S}^2(f)} \qquad 2.5.5$$

where "m" is the number of blocks used to calculate the mean value.

2.6 Data Windows

In Section 2.1, a class of spectral estimates was defined (2.1.10) which introduced the concept of data windows. A data window can be viewed as a device which allows calculating the Fourier integral transform,

$$\hat{u}(f) = \int_{-\infty}^{\infty} u(t)e^{j2\pi ft}dt \qquad 2.6.1$$

from a sample record of finite length. The effect of the data window, d(t) on the estimate $a_T(f)$ can be investigated, after a brief statement of the convolution theorem.

The convolution theorem states that the Fourier integral transform of the product of two time functions is equal to the convolution integral of the Fourier integral transforms of the two functions in the frequency domain. Mathematically, this may be expressed as follows.

$$\int_{-\infty}^{\infty} h(t)g(t)e^{j2\pi ft}dt = \int_{-\infty}^{\infty} \hat{h}(f)\hat{g}(f-f')df' \qquad 2.6.2$$

Where $\hat{h}(f)$ and $\hat{g}(f)$ are the integral Fourier transforms of h and g, respectively.

$$\hat{g}(f) = \int_{-\infty}^{\infty} g(t)e^{j2\pi ft}dt \qquad \hat{h}(f) = \int_{-\infty}^{\infty} h(t)e^{j2\pi ft}dt \qquad 2.6.3$$

From the definition of the estimate of the Fourier transform of u(t),

$$\hat{a}_T(f) = \int_{-\infty}^{\infty} d(t)u(t)e^{2\pi ft}dt \qquad 2.6.4$$

by the convolution theorem:

$$\int_{-\infty}^{\infty} d(t)u(t)e^{j2\pi ft}dt = \int_{-\infty}^{\infty} \hat{d}(f)\hat{u}(f-f')df' \qquad 2.6.5$$

where $a(f)$ is the true Fourier integral transform of u(t). The effect of the data window is to alter the estimate $a_T(f)$ by an amount which could be calculated using Equation 2.6.5. This relationship can be used, therefore, to find data windows whose Fourier transform $\hat{d}(f)$ which, when convolved with the true Fourier integral transform, provide an estimate of the Fourier transform, $a_T(f)$, which is close to the true value, $a(f)$.

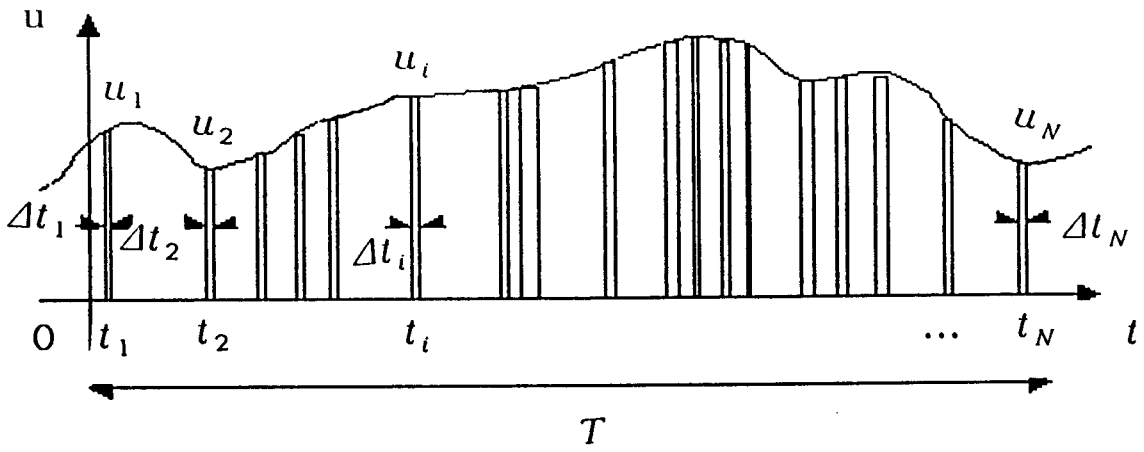

Figure 2.2.1
The Discontinuous Record u0(t)

Chapter 3: EXPERIMENTAL FACILITY

An experimental procedure was conducted to measure the power spectral density of a turbulent flow using a laser Doppler anemometer system and an axi-symmetric free jet. Following is a description of the hardware used and a discussion of relevant experimental considerations.

The following components comprised the majority of the hardware used in this investigation: jet, seeding, enclosure, LDA optics, LDA signal processor, interface and computer. Various extra hardware was used, at one point or another, for comparison and testing. This included: a Dantec model 55M Series Constant Temperature Anemometer, a Phoenix A/D converter, PDP-11/73, VAX, and micro-VAX computers, a Nicolet Semi-Ubiquitous FFT Spectrum Analyzer, a Dantec 55L90a Counter Processor and 55N10 Frequency Tracker, a Wildfire Buffer Interface, and hot wire calibration facility. See Figure 3.1.1 for a picture of the experimental facility.

3.1 Jet

An axi-symmetric free jet was manufactured for this investigation. It consisted of a blower at one end attached to a long plexiglass tube (11.2 cm inner diameter, 50 cm length) which was filled with flow straighteners to reduce the turbulence intensity at the jet exit. The jet exit velocity was fixed at 17.76 m/s with less than 0.5% turbulence intensity. The jet exit diameter of 2.8 cm and air kinematic viscosity of 15 x 10^{-6} $m^{2/s}$ produce a Reynolds Number of approximately 30000. Measurements were carried out 10 diameters downstream of the jet exit, on the centerline and at various radial positions.

3.2 Seeding

Seeding for the air was provided by glycerine smoke produced using a variable power heating rod inserted into a beaker of liquid glycerine. The glycerine particle diameter is estimated to be in the range 1-5 microns.

The seeding density in the facility could be controlled using the variable power heating rod. By increasing power to the heating rod, the concentration of glycerine smoke increased. The variable seeding density provided an adjustable system data rate in the range 0.5-20 kHz. Most measurements were carried out with a mean data rate of approximately 5 kHz. This value was selected as the maximum data rate at which continuous data collection could be accomplished with a relatively constant data rate at off-axis positions. See Figure 3.2.1 for a picture of the seeding generating equipment and the free jet.

The size and the mass of particles used to trace the flow can limit the highest frequency which can be measured. The particles operate in Stokes' regime and can be shown to respond like a first order filter with an attenuation frequency dependent on particle size. For the glycerine/water particles used in the size range of 0.1 - 1.0 μm the frequency response is estimated at 10 kHz in air, Buchhave (1979).

Another aspect of the LDA seeding principle which may limit frequency response is the finite duration of time it takes particles to cross the measurement volume. The maximum spectral resolution corresponds to the inverse of the average particle residence time. For the present investigation the average residence time is approximately 5μs which corresponds to a frequency response of 200 kHz.

3.3 Enclosure

The room in which the experiment was performed was very large. In order to insure uniform seeding and a sufficiently high seeding density, the experimental facility was enclosed by plastic sheets. The facility so obtained measured approximately 5m x 5m by 2m height and the jet was placed such that the measurement section was located near the center of the enclosure. The plastic sheets are evident in Figure 3.1.1. As a safety precaution, a "gas mask" was used when working in the highly seeded enclosure, see Figure 3.3.1.
The seeding generator was allowed to run continuously during the measurements to assure a high seeding density of statistically uniformly distributed particles.

3.4 LDA Optics

The laser Doppler anemometer used was a He-Ne based single channel system with frequency shift configured in forward scatter. The front lens focal length was 310 mm and the beam separation 50 mm which combine to yield a calibration factor of 3.12 ms^{-1} / Mhz. Laser power was 10 mw. The forward scatter configuration contributed a ten fold higher data rate compared to that obtained in backscatter. Beam expansion of 1.95 X was used. The optical specifications listed yield a measurement volume dimension of: .16 x .16 x 1.3 mm (on-axis component.) The orientation of the LDA measurement volume relative to the jet is indicated in Figure 3.4.1.

3.5 LDA Signal Processor

Measurements were taken using a Dantec model 57N10 Burst Spectrum Analyzer (BSA) signal processor interfaced to an IBM AT compatible computer. This signal processor determines the Doppler frequency using

a hard-wired FFT technique. The BSA also measures the particle arrival and residence times. The conventions used by the BSA for measuring and representing these measured values is described in the Dantec 57N10 Burst Spectrum Analyzer Instruction Manual. They will be summarized here.

The Doppler frequency f_D is resolved over the operating bandwidth BW ("span") by a binary number, V_{bin}. V_{bin} depends on the record length (or number of samples used by the signal processor to perform the FFT on) by:

$$f_D = f_c - \frac{1.5BW}{2} + V_{bin} \frac{1.5BW}{2^{11+R_L}} \quad . \qquad 3.5.1$$

where, f_c is the center frequency, R_L is an integer equal to: 0, 1, 2, 3, when the number of samples selected (record length,) R_1 is: 8, 16, 32, 64, respectively. This expression shows that velocity resolution increases with increasing record length and that the maximum resolution (14 bits) is obtained when R_1 is equal to 64.

The BSA also determines the particle residence time and arrival time. The residence time is measured using an accumulator incrementing at a clock frequency equal to half the processor's sampling frequency. The sampling frequency f_s, is bandwidth dependent, $f_s = 1.5$ BW . The residence time is represented by a 12 bit binary number. The arrival time measurement is absolute. It is made using a free-running 14 bit register incrementing at frequency, F_s equal to the sample interval (or sample frequency divided by the record length,) $F_s = f_s / R_1$. The arrival time is represented by a 14 bit binary number.

As can be seen by examining the above relations, a trade-off exists between Doppler frequency resolution and arrival and residence time resolution. For this investigation a compromise was made, sacrificing velocity resolution to achieve greater time resolution. The bandwidth, BW was fixed at 8 Mhz and the record length, R_l maintained at 32. This yields a sample frequency, f_s of 12 Mhz, an arrival time clock frequency F_s of 375 kHz, (2.6μs resolution), a residence time clock frequency of 8 Mhz, (125 ns resolution), and Doppler frequency resolution of 8 Mhz / 2^{13} (approximately .001 MHz.) Data was collected while varying the arrival time clock frequency to see what effect the changing arrival time resolution had on the results.

The frequency response of a laser Doppler anemometer system is usually limited by the signal processor. The BSA signal processor works on a digital principle able to measure step-changes in velocity; it has infinite slew rate and therefore can be considered to have near-infinite frequency response or dynamic range.

3.6 Interface and Computer

The BSA signal processor comes equipped with an industry standard IEEE interface. This was interfaced to the IBM AT compatible computer via a National Instruments PC IIA GPIB Interface. The drivers for these interfaces are included in the standard software supplied by the manufacturers. The maximum data throughput for the IEEE interface is specified at 300 kb/s which translates to 50 ksamples of data/s. Each sample consists of 6 bytes.

The computer was equipped with 640 kb RAM, 8087 floating point chip, 1.2 Mb floppy disk drive, 20 Mb hard disk, and EGA graphics adapter.

Software was written in Ryan-McFarland FORTRAN 77. Figure 3.6.1 shows the BSA signal processor and IBM AT compatible computer which were used.

3.7 CTA System

The constant temperature anemometer (CTA), is an analog device with a frequency response limited by the feedback loop which maintains the probe at constant temperature. This limit depends on the cable length, the probe type, the AC gain and many other factors. Fortunately, the CTA frequency response is adjustable by the incorporation of a "square-wave test" function built into the device. By adjusting the bridge arm inductance and capacitance while simultaneously increasing the AC Gain and Filter settings, it is possible to optimize the frequency response of the system. The CTA was adjusted to a frequency response exceeding 150 kHz, as measured by the oscilloscope used during the square-wave test. This value is considerably higher than the frequency cutoff imposed by the spatial resolution of the wire. For this investigation, this value is 25 kHz at the centerline, and about 2.5 kHz at the largest radial location. See Section 5.6. This is still well above the frequencies of interest here.

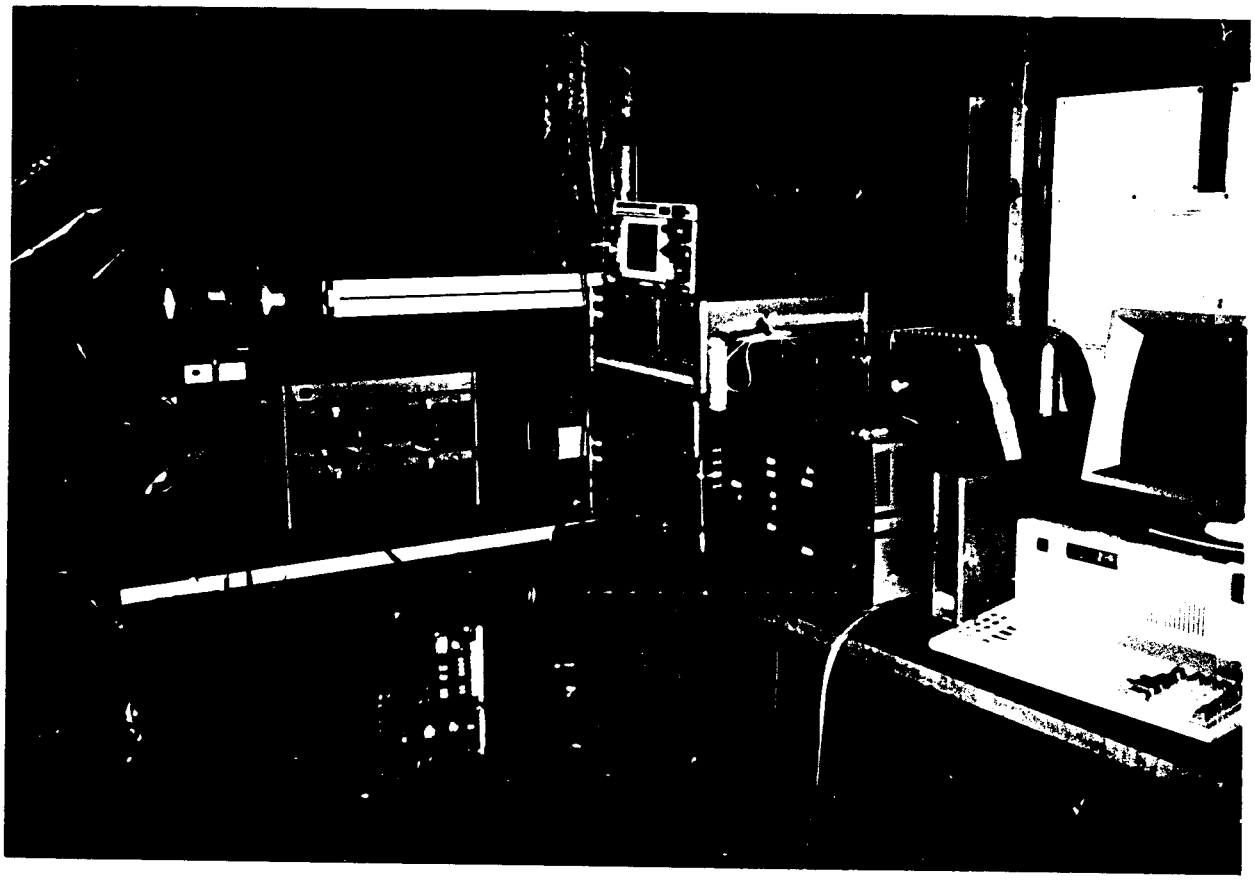

Figure 3.1.1

The Experimental Facility

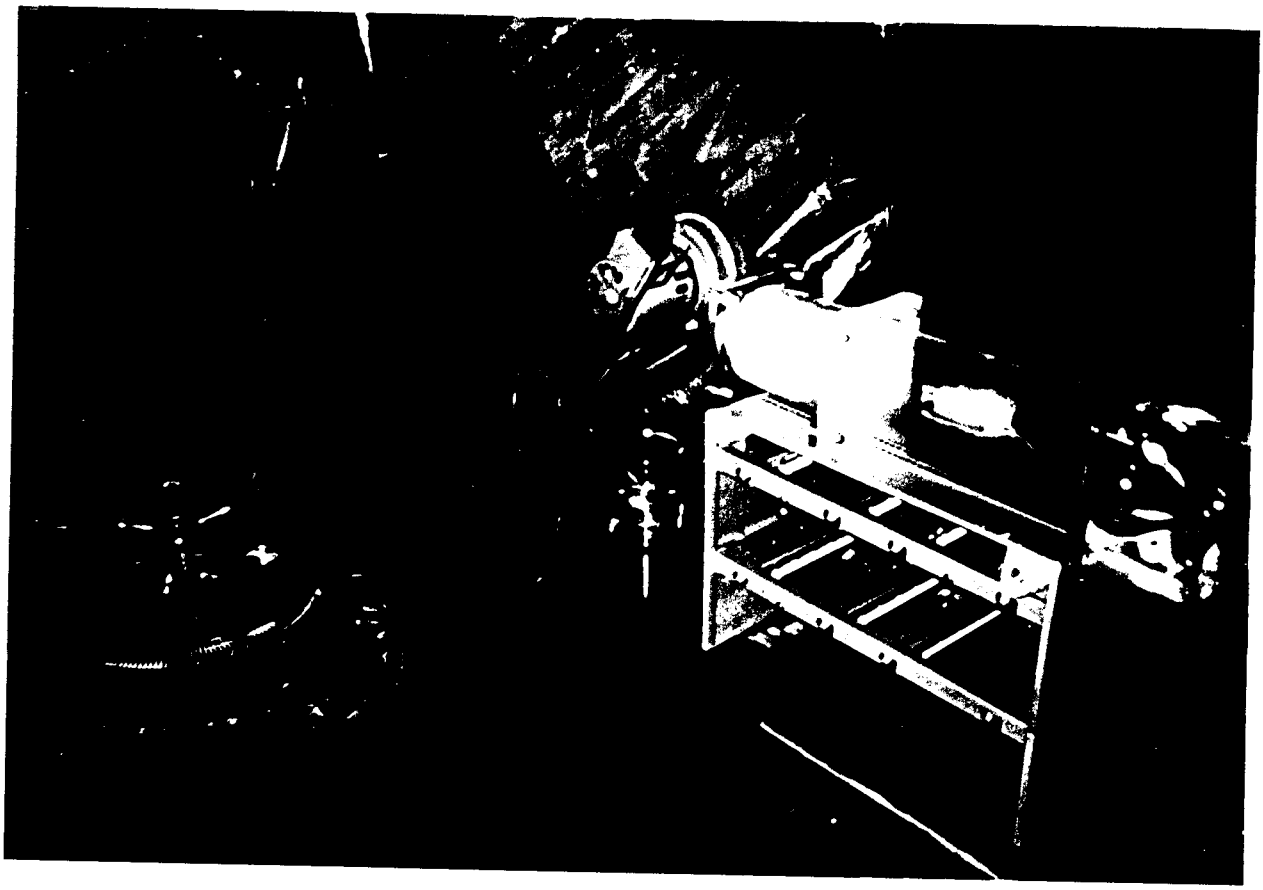

Figure 3.2.1
The Seeding Generator and Free Jet

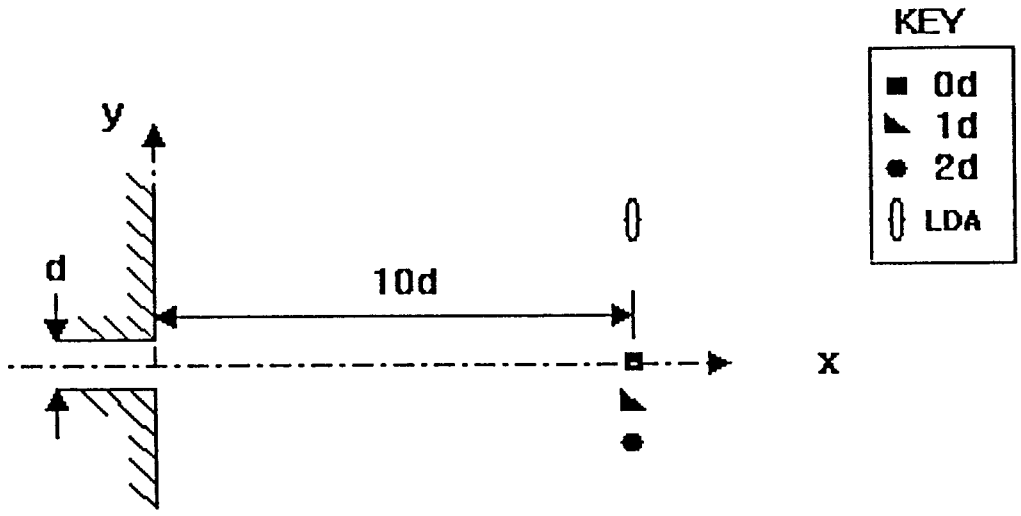

Figure 3.4.1
Jet Coordinate System, Measurement Positions,
and LDA Measurement Volume Orientation

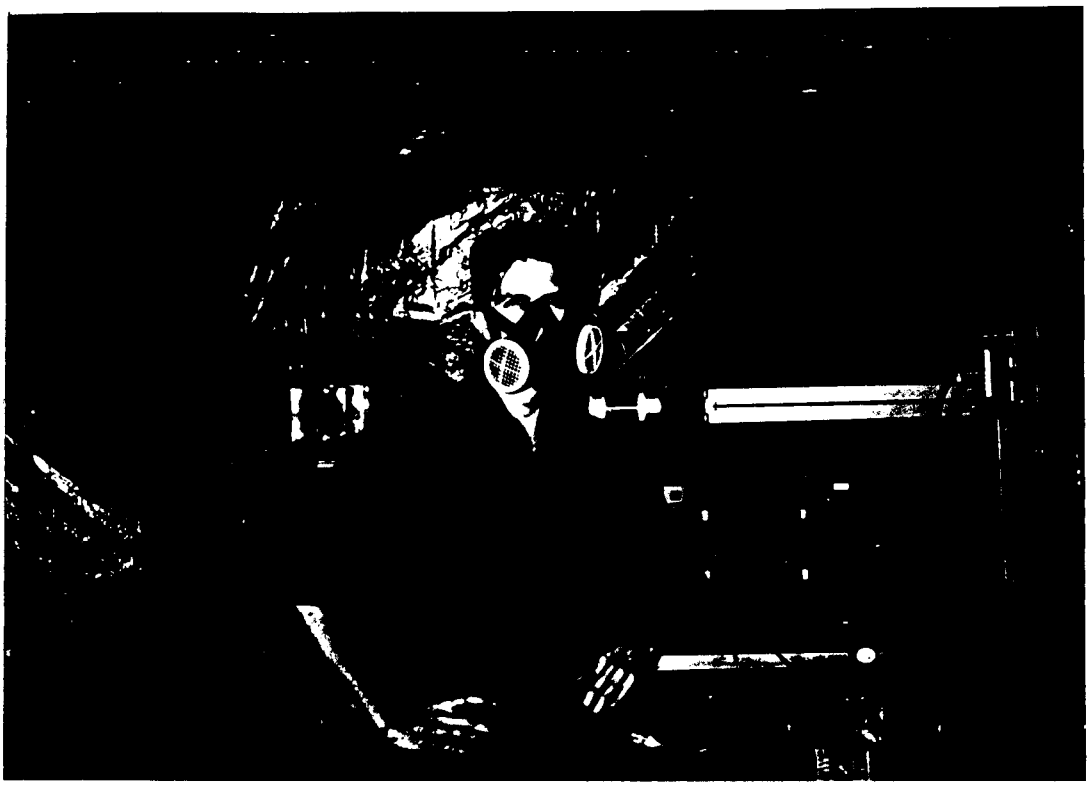

Figure 3.3.1
Safety Precautions for High Seeding Density Conditions

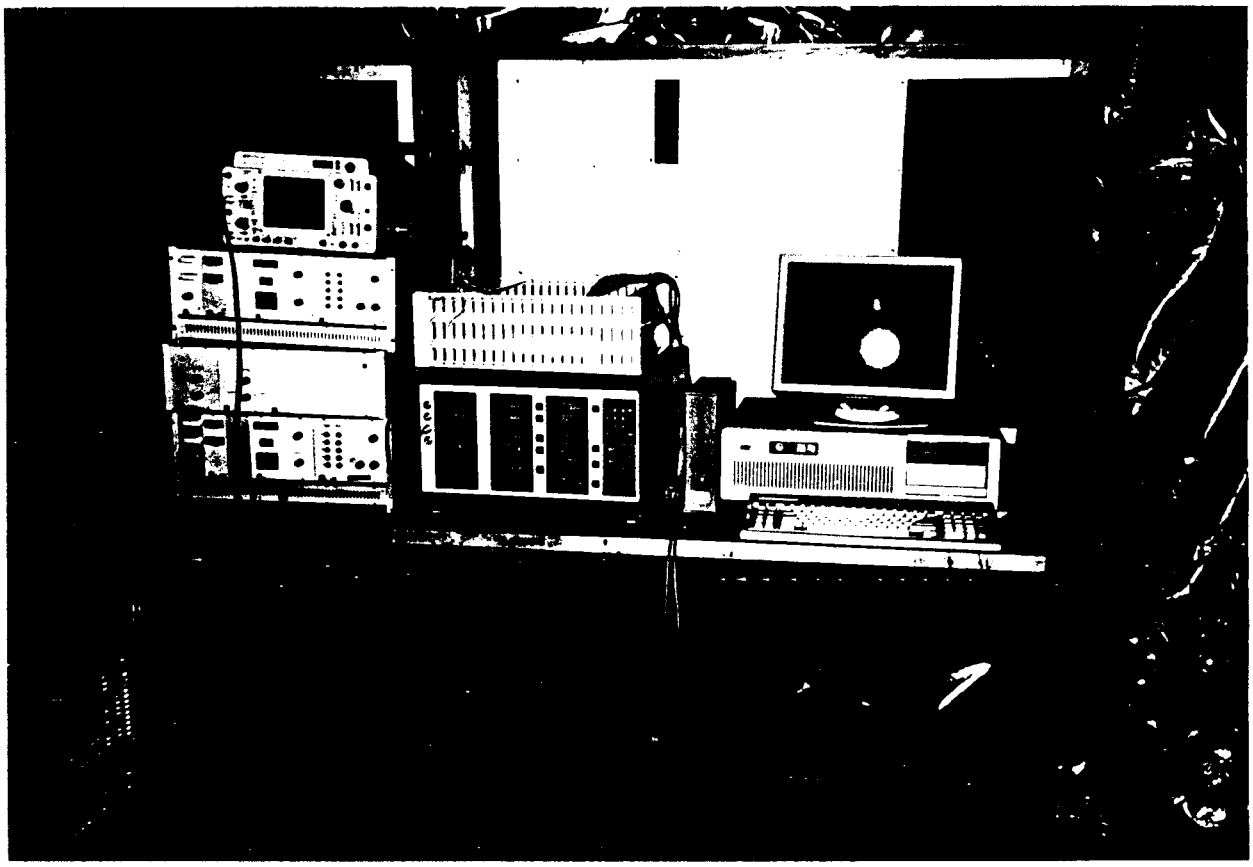

Figure 3.6.1
Signal Processing Equipment

Chapter 4: SOFTWARE

The software required for testing the algorithm consisted of commercially available programs, archival programs, and custom-made programs for calculation of biased and unbiased power spectral density.

Data Acquisition and storage was carried out using the standard Dantec BSA software. A conversion routine, DATCV, provided by Dantec, converts the binary raw data to "physical variables" (i.e.: m/s) in ASCII format. The spectral analysis routine operates on this converted data file.

In addition to the above programs, others were used or written for various reasons. These include a battery of programs created by the Turbulence Research Laboratory at SUNYAB:

IDSL, a driver for the Wildfire Buffer Interface,

RECDAT, a data acquisition program used in conjunction with the PHOENIX A/D Converter,

PWSPEC, an FFT routine for calculating the unbiased spectral estimate and block averaging of data obtained using RECDAT,

CALIB1, a hot-wire calibration and linearization program, and

TRLPLOT, a graphics program which runs on the VAX over a DECNET line and produces graphics plots on the Tektronix terminal or VT100 Laser Printer.

Other software which was written includes:

PLOTL a program to plot the power spectral density as a log-log or semi-log plot,

MAINC a modified version of MAIN4 to process files of equispaced data for test purposes. See the following sections for a detailed description of the spectral analysis routine.

4.1 Description of the Spectral Analysis Routine

A data processing scheme (Rapid Recursive Spectral Analysis Algorithm) was implemented to calculate the biased and unbiased power spectral density (equations 2.2.8, and 2.3.1) of the fluctuating (single) velocity component, u_i, (i = 1, 2, 3, ... N) measured by the LDA. The algorithm utilizes digital outputs from the LDA signal processor. These outputs are: Doppler frequency, f_{di}, residence time, Δt_i, and arrival time, t_i of the i randomly spaced samples in the block of length, T. The velocity component u_i is calculated from the Doppler frequency, f_{di}, using $u_i = C\ f_{di}$, where C is the calibration factor (see Section 3.4.)

Some flexibility has been incorporated into the routine to make it more user-friendly. For example, the user can select the harmonic frequencies f_k, ($f_k = k/T$, k = 1, 2, 3, ... F), and the block averaging time, T. A recursive relation is used to speed up computation time and a data window is applied in the time domain to decrease high frequency digital noise. A plotting routine is called after successive block averages to provide qualitative investigation of the spectrum and to display other important system parameters: name of raw data file, total number of samples in the file, total samples processed, samples in current block, and actual duration of current block. A detailed description of the program and flow chart is given below. The major segments of the program are:

i) MAIN4; the main program, which sequentially reads blocks of data and averages the spectral estimate obtained with results from previous blocks,

ii) SPEC4; a subroutine, which calculates the spectral estimate, $S_T(f_k)$.

iii) PLOT4; a plotting routine which sequentially plots block averaged results. This gives an indication of convergence of the spectrum and an indication of suspicious results.

4.2 Flow Chart

Refer to the flow chart in Figure 4.2.1 for the following discussion of the spectral analysis routine.

The user initially sets the parameters: block averaging time, T (in seconds); upper harmonic frequency, F (dimensionless); "mode" of harmonic frequency spacing, and harmonic frequency interval, DF (dimensionless.)

The term harmonic frequency is used to differentiate from physical frequency (in Hertz.) To convert from harmonic frequency to physical frequency it is necessary to divide harmonic frequency by the block averaging time, T. The harmonic decomposition of the record (of length T) requires breaking it into integral segments the inverse period of which is the harmonic frequency, k = 1, 2, 3, ... F. These harmonic frequencies correspond to the physical frequencies, f_k = 1/T, 2/T, 3/T, ... F/T.

When the block averaging time is 1 second, the harmonic frequency is equal to the physical frequency. In the general case, T does not equal 1 second, therefore, the following transformation is necessary in calculating $S_T(f_k)$:

$$S_T(f_k) \leftarrow S_T(k) \qquad 4.2.1$$

$S_T(f_k)$ is the spectral estimate at physical frequency f_k, $S_T(k)$ is its

harmonic equivalent. See Section 4.3 for details.

The spectral resolution of the power spectral density calculated on the basis of a data record of length T is: 1/T. Therefore, spectral resolution increases with block averaging time, at the expense of block number, "M" for a run of fixed total length.

The data record consists of velocity, residence time, and arrival time. The arrival time can be used to determine the beginning and end of blocks. Since particle arrival time is random, there is a small difference between the actual block length, T_m and the selected block length, T. However, since the inverse average data rate is small compared to the block length, this difference is negligible.

Note, that most spectral analysis routines operate on blocks of fixed record length. This is a natural consequence of the fact that most spectral analysis routines operate on equispaced data, and fixed sample number corresponds to fixed record length. When the sampling rate is random, (as in LDA measurements) fixed sample number corresponds to random block length. Spectral analysis of blocks with different record lengths leads to various problems. In the present investigation, it would cause spectral estimates to be calculated at random (i.e.: not fixed) frequencies, which would be difficult to average. Also, distinguishing the effect of insufficient record length (discussed in Section 7.3) would be very difficult if the record length changed. For these reasons, throughout the investigation, calculations were performed on blocks of data of fixed record length.

Some important notes concerning the program source code are injected here. The block of converted data is stored in three vectors U, T, and

DT in the main program. These arrays are dimensioned to 5028. This limits the combination of block length and data rate (N) to 5028. The converted data includes "false records" from the signal processor. These records correspond to arrival time overflows ("ATO's") which are ignored when reading sequential strings of valid data.

The calculation of $S_T(f_k)$ will be discussed fully in section 4.3. However, it is useful to write the expression (4.2.1) for $S_T(f_k)$ explicitly:

$$S_{Tm}(f_k) = \frac{T_m}{\left(\sum_{i=1}^{N} \Delta t_i\right)^2 - \sum_{i=1}^{N} \Delta t_i^2} \{ | \sum_{i=1}^{N} d_i u_i \Delta t_i e^{j2\pi f_k t_i} |^2 - \sum_{i=1}^{N} (d_i u_i \Delta t_i)^2 \}$$

$S_{Tm}(f_k)$ is the spectral estimate calculated from the "m^{th}" block of data and has units [m^2/s], $f_k = k/T$ is frequency [Hz], "i" is the i^{th} particle in the block (which resets after each block), u_i is the velocity component [m/s], t_i is the arrival time [s], N is the number of samples in the block [ ], Δt_i is the residence time [s], T_m is the length of the m^{th} block [s], d_i is the data window [ ], and m = 1, 2, 3, ... M. Note, that this algorithm uses a single summation and therefore differs from the one used by Buchhave (1979) which incorporated a double summation. This was discussed fully in Section 2.2.

There are two modes of program operation: fixed and variable. These modes distinguish the variation in harmonic frequency spacing, as follows:

mode = FIX: $k = 1, DF, 2DF, 3DF, \ldots F$ 4.2.2

mode = VAR: $k = DF^0, 2DF^0, 3DF^0, \ldots (DF-1)DF^0,$

$DF^1, 2DF^1, 3DF^1, \ldots (DF-1)DF^1,$

$DF^2, 2DF^2, 3DF^2, \ldots F$ 4.2.3

Notice the function of the harmonic frequency interval, DF. In fixed mode DF is the fixed spacing between harmonic frequencies. Since F is the maximum harmonic frequency, in fixed mode the number frequencies at which Fourier Coefficients will be calculated is (F/DF) + 1. (The variation of k differs when DF = 1. In this case, k = 1, 2 ,3 ... F.)

In variable mode, the spacing between harmonic frequencies varies. The harmonic frequency spacing is constant "DF" times, after which the harmonic frequency increases by squaring itself. It is easier to understand the function of DF in variable mode by using an example. Let DF = 10. In variable mode, the harmonic frequencies used will be : k = 1, 2, 3, ... 9, 10, 20, 30, ... 90, 100, 200, 300, ... 900, 1000, 2000, 3000, ... 9000, 10000, 20000, ... F. Variable mode allows logarithmically spaced intervals to be used in the calculation of power spectral density. A minor note should be inserted: the program limits the number of times that the harmonic frequency will square itself before reaching F. This limit is 4.

The data window, d_i is used to improve the spectral window associated with the spectral estimate. Data windows are employed to reduce the effect of finite duration sample intervals on calculations of power spectral density. As previously described, the data window is a boxcar

function with unit amplitude: $d_i = 1$, $i = 1, 2, 3, \ldots N$. Since multiplication by unity does not effect the calculations, the data window is included only to maintain the generality of the development.

After $S_T(f_k)$ has been calculated from the m^{th} block using equation 4.2.1, the results are averaged with the results from previous blocks by ensemble averaging. This procedure continues until the end of the data file, after which, the results of the block averaged power spectral density calculation are stored for analysis.

4.3 The Rapid Recursive Relation

The calculation of $S_T(f_k)$ does not entail the straightforward evaluation of equation 4.2.1. As previously noted, a recursive relation ("Rapid Recursive Fourier Transform") is used to speed up computation time. Therefore, the calculation of $S_T(f_k)$ is slightly modified.

"Rapid Recursive Factors," M_i are used to calculate $\hat{u}_{0T}(k)$,

$$\hat{u}_{0T}(k) = \sum_{i=1}^{N} c_i M_i^k \qquad 4.3.1$$

$$c_i = d_i u_i \Delta t_i \qquad 4.3.2$$

$$M_i^k = e^{j2\pi k t_i / T} \qquad 4.3.3$$

which are in turn used to calculate $S_T(f_k)$,

$$S_T(k) = \frac{T}{\left(\sum_{i=1}^{N} \Delta t_i\right)^2 - \sum_{i=1}^{N} \Delta t_i^2} \left\{ |\hat{u}_{0T}(f_k)|^2 - \sum_{i=1}^{N} (d_i u_i \Delta t_i)^2 \right\}. \qquad 4.3.4$$

Finally, $S_T(k)$ is converted from harmonic to physical frequency.

$$S_T(k/T) \leftarrow S_T(k) \qquad 4.3.5$$

The recursive relation will be explained further. Let, $M_i(f_k) = e^{j2\pi f_k t_i}$ where, $f_k = k/T$.

Incorporate the following notation: $M_i(1/T) = M_i^1 = e^{j2\pi t_i/T}$

$$M_i^k = e^{j2\pi k t_i/T}. \qquad 4.3.6$$

In fixed mode notice that, $M_i^{nDF} = M_i^{(n-1)DF} M_i^{DF}$. 4.3.7

That is, the quantity, $M_i^{nDF} = e^{j2\pi n(DF)t_i/T}$ for $n>1$ can be calculated by multiplying the quantity $M_i^{(n-1)DF}$ which has already been calculated, by $M_i^{DF} = e^{j2\pi DF t_i/T}$.

The calculation of M_i^{nDF} is then used to calculate $M_i^{(n+1)DF}$ until k = F.

The recursive calculation is more complicated in variable mode. Notice that relation 4.3.7 (for fixed mode) can be employed "DF" times in variable mode, during intervals which have fixed harmonic spacing (i.e.: during decades.) For the intervals in which that isn't true (i.e.: between decades), the definition 4.3.3 is employed to calculate M_i.

The following expression shows how the recursive relation is implemented in variable mode:

$$M_i^{nDF^x} = M_i^{(n-1)DF^x} M_i^{DF^x} \qquad n \neq 1 \qquad 4.3.8$$

$$M_i^k = e^{j2\pi k t_i/T} \qquad n = k = 1 \qquad 4.3.9$$

In the above equations, x is any arbitrary number equal to 1, 2, 3, or 4.

The combination of the Rapid Recursive Fourier Transform and the use of variable spaced frequency intervals optimizes the speed of calculation of $S_T(f_k)$.

Figure 4.2.1
Flow Chart of The Rapid Recursive Spectral Analysis Routine

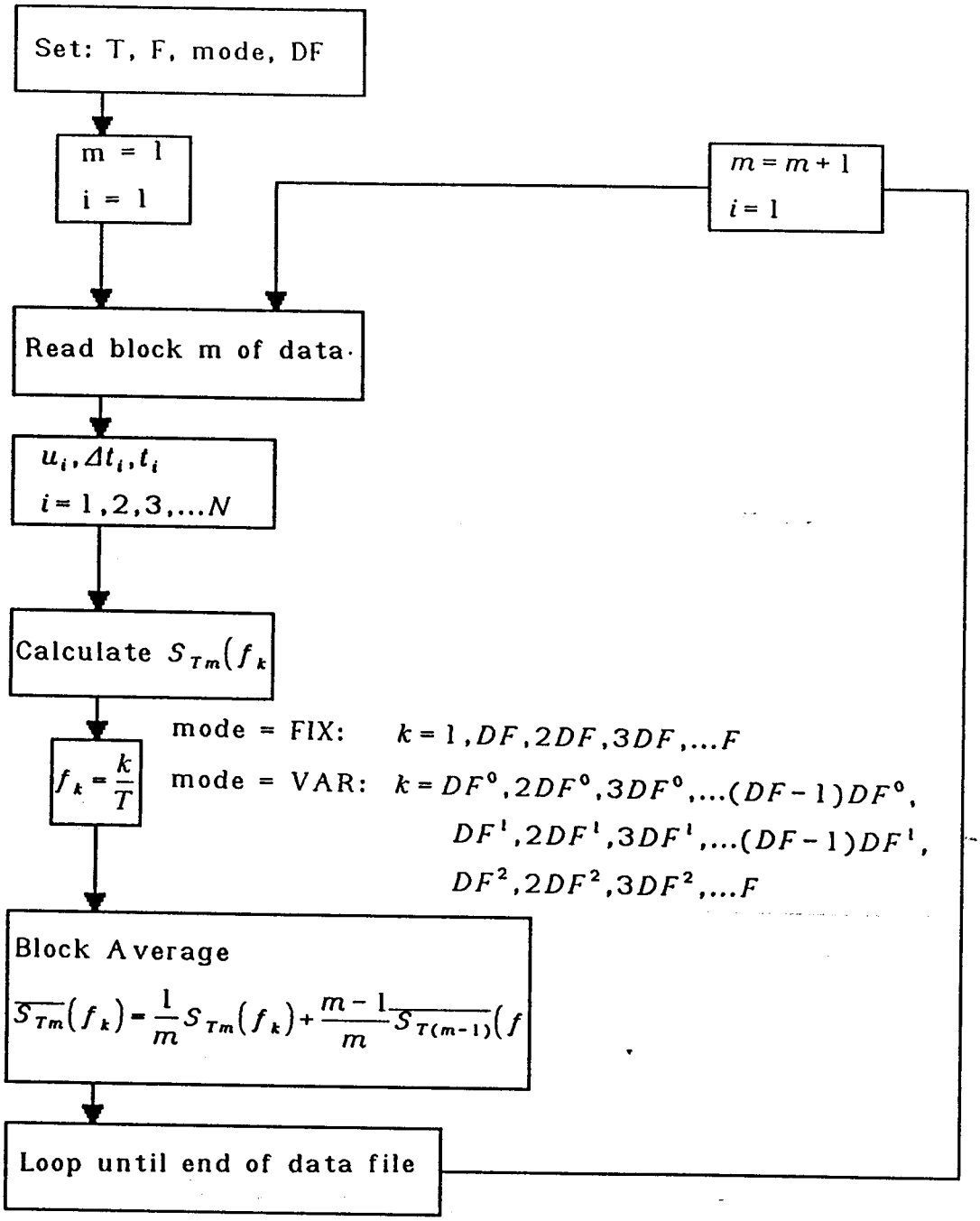

Chapter 5: PROCEDURE

Following is a description of the procedure used to conduct the experiments with a discussion of the most important experimental considerations involved.

5.1 Optical Alignment

The He-Ne LDA system must be aligned before use. The technique used to align the optics is a standard procedure available from any of the commercial manufacturers of LDA equipment. In summary, the procedure entails the adjusting two laser beams to become parallel. Once focused, the beams should intersect at the measurement volume. The receiving optics, configured in forward scatter must then also be adjusted. The receiving optical unit is equipped with a variable focusing lens which must be placed a minimum distance of 600 mm from the intersection before focusing. The unit must be adjusted such that the image of the focused intersection passes through a pinhole into the photo-multiplier (PM) tube. Once this is accomplished, the transmitting and receiving optics are properly aligned.

5.2 Signal Processor Adjustment

Preliminary measurements were taken with the LDA measurement volume located at an appropriate test point. At this time seeding density and electrical controls are adjusted to optimize data collection. A quantifiable indicator of the signal quality is provide by the validation meter on the front of the signal processor. The filtered and amplified Doppler burst signal is available for qualitative judgement of signal quality using an oscilloscope. Filter settings, amplifier and PM tube gain, and frequency shift controls provide the most critical

control over the quality of the monitor output signal. These controls were adjusted until the monitor output signal was clean with no filter clipping evident. Filter clipping can be determined by using the on-line histogram included in the data acquisition software. Once the frequency shift is adjusted to provide sufficient zero crossings of the Doppler burst with no filter clipping and sufficient validation and data rate, the system is ready to operate.

5.3 Measurement Volume

The laser Doppler anemometer front lens focal length was 310 mm, beam separation was 50 mm, beam expansion was 1.95 X. These optical specifications along with the dimension of the laser beam from the manufacturer yield an LDA measurement volume dimension of: .16 x .16 x 1.3 mm, with the orientation indicated in Figure 3.4.1.

The measurement locations used in this investigation are indicated in Figure 3.4.1. One centerline and two off-axis positions were used, at a downstream location of 10 jet diameters. The measurement position was determined using a laser beam to identify the jet centerline, and a plumb-bob to determine the downstream and radial coordinates. A traversing mechanism fitted with a vernier adjustment was used to accurately position the hot wire probe.

5.4 Data Rate

With the optics aligned, the signal processor settings optimized, and the LDA measurement volume positioned at the test point, the system data rate can be adjusted. The seeding density and signal processor gain are the most important parameters affecting the data rate. For this

investigation the data rate was maintained at a constant value during each run at different positions. Different runs were made at high and low data rates with short and long run times, respectively, to investigate the effect on spectral variability.

The data rate was limited in practice to a mean value of 5 khz. This was the limit at which the BSA could continuously output all measured variables over the IEEE interface without an input buffer overflow error (which would cause gaps in the data record.) Although, in principle, gaps in the record of the velocity data do not affect the direct Fourier Transform, the sequential block averaging technique implemented did not check for blocks of empty data. Therefore the possibility of encountering an entire block without data was eliminated by ensuring that data acquisition was continuous. Note that "gaps" in the velocity record could also correspond to an improper seeding technique. In practice, the software could be set up to check for gaps larger than "expected" for a given mean data rate and flag the user of a possible error condition.

5.5 Data Collection Time

The time-out limit for data collection is user controlled. As discussed above, there were certain practical limits encountered in establishing a high data rate (it was limited by the signal processor computer interface.) Similarly, other practical limits dictated the maximum data collection time, as will be discussed below.

The number of blocks used to block average the spectral estimates should be as large as possible to decrease the variability associated with the

estimate (see section 2.5.) The block averaging time should be as long as possible for maximum spectral resolution. These two considerations dictate that the total sampling time should be as large as possible.

The constraint on unlimited data acquisition time is computer storage space. Since the program does not operate "on-line", all the data which is collected must be stored. (Note, that there is no reason why the algorithm couldn't be implemented on-line, given the right processor, or by implementing parallel processing, for example.) The converted data must also be stored. For this investigation, one floppy disk of raw data (360 kbytes) requires over 3 Mbytes of hard disk storage in ASCII format. This corresponds to a total record length of about 50000 velocity samples. The number of runs, data rate, and length of a run, are severely impacted by storage requirements.

5.6 Hot Wire Data Acquisition and Processing

The seeding generator was shut off before measuring with the hot wire anemometer to eliminate the effect of the glycerine smoke on the calibration. With all other factors unchanged, 100 blocks of 0.2048 second hot wire data were taken with an A/D converter sampling the non-linearized output of the anemometer at 10 khz. The calibration curve was fit with a fourth order polynomial to convert the raw voltages to velocity. A standard block averaging FFT routine was used to calculate the half-line power spectral density (equation 2.4.1) averaged over 100 blocks. The integrated half-line spectrum compared to within 1% of half the mean square value of the velocity fluctuation calculated for the hot wire data. This test gives confidence in the results of the hot wire power spectral density, which was used subsequently for comparison with the results from the LDA.

In applications where the sampling rate is fixed, the time between samples is constant and the Nyquist Theorem applies. In these applications (i.e.: measurements made with an A/D converter,) the sampling rate limits the alias-free frequency response to $f_s/2$. When the sampling rate is random, as in the case of the LDA operated under conditions of low seeding density, the Nyquist Theorem does not apply and the frequency response is not in principle limited by the sampling rate, although the variability is affected (see Section 2.5.) From the result calculated in Section 5.9, the Nyquist criteria stipulates that the sampling rate of the A/D converter should exceed 64 kHz to resolve the Kolmogorov microscale.

If the hot wire probe is large, however, such that it cannot resolve a structure of length l_w, then it makes no sense to sample faster than d^{-1} where $d = l_w / s$ and s is the speed with which the structure is convected past the measurement point. For this investigation, the dimension, l_w of the hot wire probe ($200\,\mu m$) exceeds twice the dimension of the Kolmogorov micro-scale (η-$50\mu m$.) Therefore, it is the non-infinitesmal spacial extent of the transducer which determines the optimum sampling rate. This sample rate, f_c is given by:

$$f_c = \frac{\bar{u}}{2 l_w} \qquad 5.6.1$$

for $\bar{u}$ = 10 m/s, and l_w = .200 mm, f_c = 25 kHz. Therefore, the optimum sampling rate to be used in digitizing the analog output of the hot-wire anemometer system is 50 kHz. Obviously, a lower rate could have been used away from the centerline where the mean velocity was lower.

5.7 Experimental Variables

After collection of data using both LDA and hot wire probe, the measurement location was changed and the above procedure repeated. Typically, one on-axis and two off-axis positions were used. This constituted a single run of the experiment.

Besides varying the position (which is equivalent to altering the turbulence intensity,) other variables were adjusted during the course of the procedure. The most important of these parameters was the system data rate which was adjustable in the range 0.5 - 20 khz. Once the data rate was fixed, it was maintained constant during the course of one run. Data collection time was varied to compensate for the data rate, as subject to disk storage space as previously described.

Besides position, turbulence intensity, data rate, and sampling time, other parameters such as arrival time clock frequency, block averaging time, etc. were adjusted experimentally for verification and testing purposes. The impact of these effects on the outcome of the power spectral density calculations was examined.

5.8 Data Reduction Time

The Rapid Recursive Spectral Analysis Algorithm (RRSAA) computes the block averaged power spectral density of the turbulent velocity measured by the laser Doppler anemometer using data from randomly arriving particles. A description of the program and its functions is included in Chapter 4.

Results from the power spectral analysis of LDA data were compared with the results from the hot wire anemometer. Biased and unbiased estimates

of power spectral density were calculated and compared as a function of increasing turbulence intensity.

It may be of interest to note the time required for data acquisition and reduction (using the 8 MHz IBM AT compatible computer with 28 ms hard disk access time.) At a single position, data collection required approximately 10 seconds (although some runs lasted up to two minutes.) The amount of time required to convert from binary numbers to physical units (using DATCV) was approximately 8 minutes per 10000 samples. For a typical data file of 10 seconds, with an average data rate of 5 khz, 40 minutes are required to run the conversion routine. The spectral analysis program on the other hand has a variable run time depending on the user selected parameters, but typical values can be mentioned.

Most of the processing (using MAIN4) was performed using the following parameters: F = 1000, T = 1.0 s, DF = 10, mode = VAR. For the example under consideration, 30 frequencies are used and 30 spectral estimates calculated. The frequency resolution for this example is 1 Hz and the maximum spectral frequency 1 kHz. Since run time is 10 seconds, with T equal to 1 second, 10 blocks will be block averaged. Approximately 45 seconds are therefore required to read the first block of data, followed by 45 seconds to calculate the spectral estimate. For 10 blocks, approximately 15 minutes will be required to process the data file.

It is interesting to note that extremely fast processing of the data would not significantly reduce processing time, since most of the time (for this particular example) is consumed by computer I/O and data "pre-conversion." Increased speed could be obtained, however, by performing the calculations "on-line." The drawback of on-line processing is that the raw data is lost.

Note that if the input parameters are changed, for example setting F = 10000, DF = 1, mode = FIX, which corresponds to calculating 10000 estimates for 10 blocks of 5000 samples each, several hours will be required to process the same data file.

5.9 Estimating the Highest Frequencies To Be Measured

The highest frequency to be measured in turbulent flows of moderate turbulence intensity ($u'/\bar{u} < 1$) corresponds to the inverse time in which it takes the smallest structures in the flow to be convected past the measurement point. This frequency can be calculated by the following procedure.

The smallest spacial structures in turbulent flow are the eddies which dissipate turbulent energy in the form of heat at the Kolmogorov microscale. By Taylor's hypothesis, these structures are convected past the measurement point at the mean velocity as if frozen. This is because the turnover time of these eddies is long compared to the convection time.

The Kolmogorov Microscale η, is given by:

$$\eta = \left(\nu^3/\epsilon\right)^{1/4} \qquad 5.9.1$$

Where ν is the kinematic viscosity of air and ϵ is the turbulent dissipation.

$$\epsilon = \frac{u'^3}{L} \qquad 5.9.2$$

For the near jet, the length scale, L can be estimated according to the empirical relation $L = .07x$. u' is the rms velocity (about 25% of the mean velocity, $\bar{u}$ on the jet centerline at $x/D = 10$.)

Using the values: $\nu = 15 \times 10^{-6} m^2/s$ and $D = 028m$ yields a value: $\eta = 50 \mu m$ for the Kolmogorov microscale. The inverse turnover time, f_k of Kolmogorov structures being convected past the measurement point at mean velocity $\bar{u} = 10 m/s$ is:

$$f_k = \frac{\bar{u}}{2\pi\eta} \qquad 5.9.3$$

which for the mean centerline velocity, $\bar{u} = 10 m/s$ yields the highest frequency to be measured in the flow, $f_k = 32 kHz$.

5.10 Impact of Hardware on Residence Time Weighting

The technique of residence time weighting to correct for velocity bias has come under fire in the international community over the past several years. It is of interest to address the ambivalence which the technique has engendered and comment on the possible reasons for it.

Application of the residence time weighting technique usually requires implementation using hardware available from commercial vendors. It will be argued that the peculiarities of commercially available hardware may be responsible for the proliferation of controversy concerning residence time weighting.

Three peices of information are required to determine the unbiased (or biased) power spectral density. Let us consider the techniques used in commercially available equipment to determine these three pieces of information and show that the intricacies inherent in these techniques may be responsible for the problems plaguing widespread acceptance of the residence time weighting algorithm.

Consider first, the measurement of particle arrival time. Measurement of the arrival time of a particle can be accomplished in one of two ways: relative and absolute. In the relative mode of operation, the time between particle arrivals is measured (inter-arrival time). In the absolute mode of operation, each particle is "time stamped" relative to a free-running clock which begins at time, t = 0. We can summarize the analysis of particle arrival time measurement and its effect on residence time weighting and accuracy of measurement, in general, by stating that a fixed frequency absolute arrival time mode of operation will always produce better resolution in the measurement of arrival time than a relative arrival time mode of operation using a floating point clock whose base frequency is equal to the frequency of the absolute arrival time clock (Kotas 1987). This problem seems to have been addressed by the commercial manufacturers. For example, the BSA processor, manufactured by Dantec Electronics, Inc. incorporates an absolute arrival time technique which is superior to the older device from this manufacturer which measured inter-arrival time using a (variable frequency) floating point clock.

Consider next, the measurement of particle velocity and residence time. these two peices of information are determined using the following techniques (using the Dantec model 55L90a Counter Processor as an example).

The time of passage for a particle to cross 8 fringes in the measurement volume, P_8, is recorded. This value is divide by 8 to get the Doppler period, and inverted to get the Doppler frequency. The time of passage, P_8, is measured using a floating point clock, and output as a 12 bit number, with an 8 bit mantissa and a 4 bit exponent. The residence time is calculated on the basis of the Doppler period, by multipying it by

the number in the fringe counter. The fringe counter is an 8 bit binary number representing the number of fringes crossed by the particle as it crosses the measurement volume. Unfortunately, the fringe counter in the 55L90a Counter Processor overflows at 256 fringes, and gives no indication of this overflow to the user. Whenever the fringe number exceeds 255, therefore, the residence time determined by this signal processor will be greatly in error. Although the Doppler frequency calculation is still correct, and therefore, the velocity is valid, the residence time which is used to implement the residence time weighting algorithm will be severely in jeopardy. Capp (1983) points out that this is a major consideration in all applications of LDA measurements at low velocity.

It should again be pointed out that the flaw inherent in this signal processor has been corrected in the Dantec 57N10 Burst Spectrum Analyzer (see Section 5.2). In addition, there exist a limited number (one?) of 55L90a Counter Processors which have been modified by Dantec (George 1988).

In conclusion, we have examined the hardware in common use for implementing the technique of residence time waiting and have examined how the representation of the data influences the results. Although it may seem presumptious to blame the suspicion regarding residence time weighting on commercially available hardware, the arguments presented certainly tend to support that argument.

Chapter 6: RESULTS

6.1 Characteristics of the Unbiased Power Spectral Density

Characteristics of the unbiased power spectral density are evident in the results presented in Figures 6.1.1 through 6.1.5. Preliminary tests of the Rapid Recursive Spectral Analysis Algorithm included; analysis of a known signal with variably modulated Doppler frequency, and adaptation of the program for hot wire anemometer data. These tests proved successful. For the later test results, see Figure 6.1.1. The test conditions in this figure correspond to a jet centerline position at x = 10 D, 25% turbulence intensity. The two results differ slightly because the hot wire results were block averaged 100 times and the LDA results were only block averaged 10 times. When the two sets had the same number of blocks used for averaging, the two results were identical.

Referring to Figure 6.1.2, (which is a log-log plot of the power spectral density comparing the unbiased estimate with the hot wire FFT estimate) notice that the LDA power spectral density (unbiased spectral estimator) agrees with the hot wire power spectral density (HWFFT estimator) to several hundred Hertz, after which, a wide disagreement is apparent.

Representation of the power spectral density on a log-log plot may be misleading. The same data presented on a log-log plot in Figure 6.1.2 is presented on a semi-log plot in Figure 6.1.3. Here the slight deviations between the two curves at high frequencies are not as apparent. The quantitative agreement of the measurements here appears excellent to frequencies extending into the kiloHertz range.

Figure 6.1.4 again reflects the quantitative agreement between the measured hot wire power spectral density (HWFFT) and the unbiased power spectral density estimate (direct transform.) Here the two techniques both clearly distinguish the on-axis and off-axis power spectral density, showing a higher peak for the off-axis position (higher turbulence intensity), and a more rapid decay with frequency compared to the on-axis position (lower turbulence intensity.) The same data is presented in Figure 6.1.5 on a semi-log plot where the agreement is good to several kiloHertz.

Generally, the unbiased power spectral density integrated to within 1% of half the mean square fluctuation and showed excellent agreement with the hot wire anemometer measurements to several hundred Hertz. For the results presented, the range of the unbiased power spectral density spanned more than two decades.

Figure 6.1.1

Test of Direct Transform on Equispaced Data

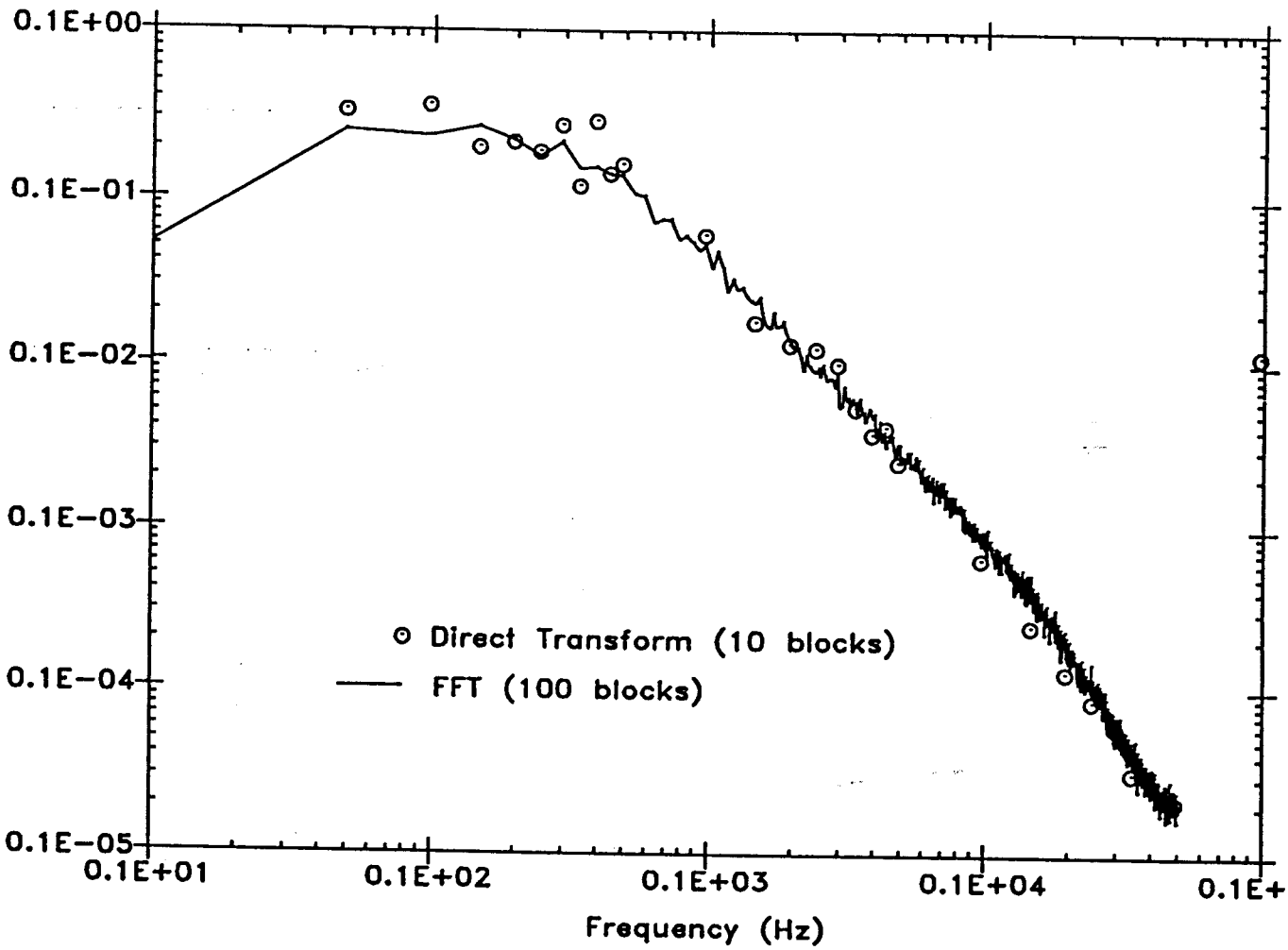

Figure 6.1.2

Comparison of Hot Wire and LDA Power Spectral Density (Log-Log Plot)

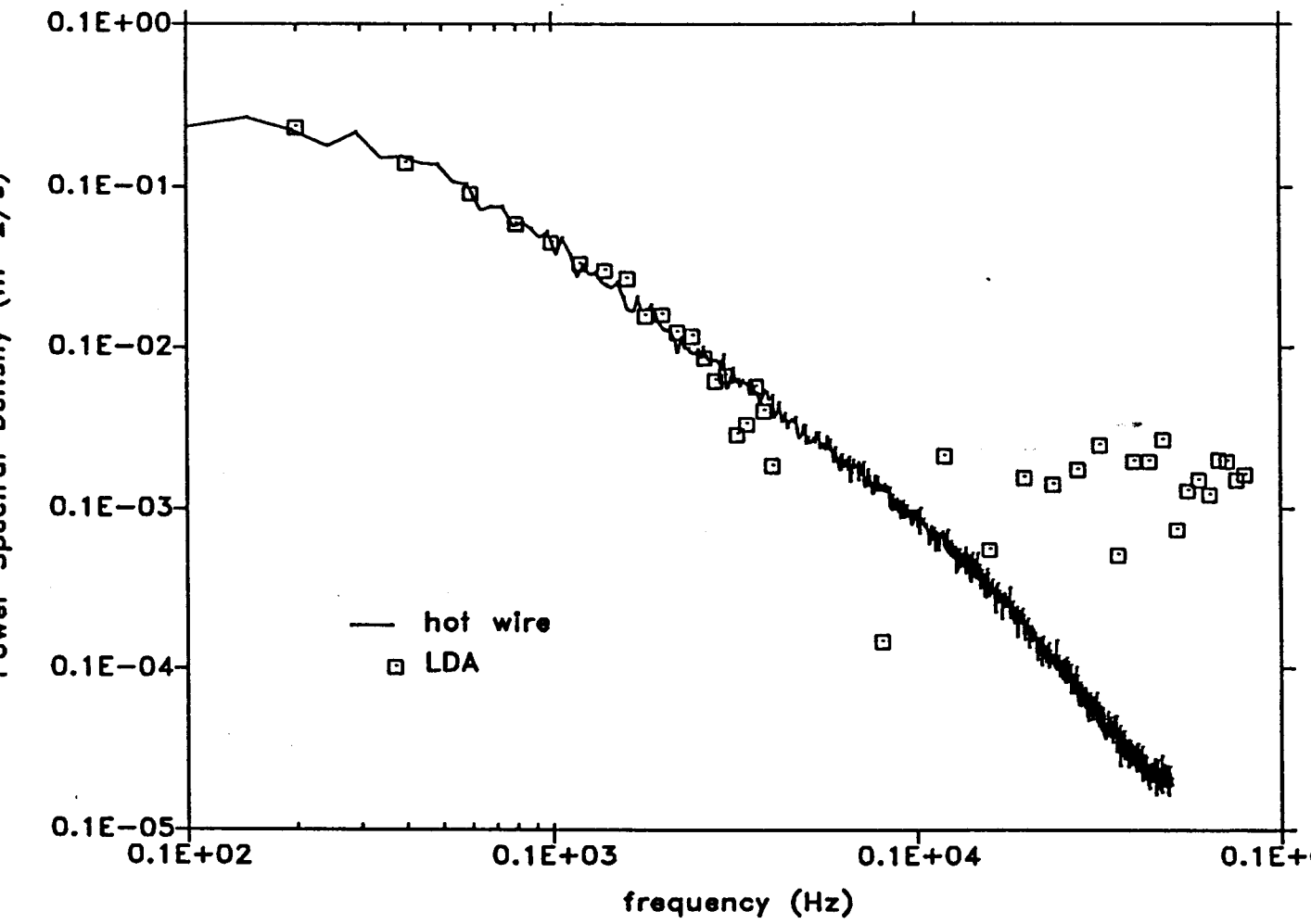

Figure 6.1.3

Comparison of Hot Wire and LDA Power Spectral Density (Semilog Plot)

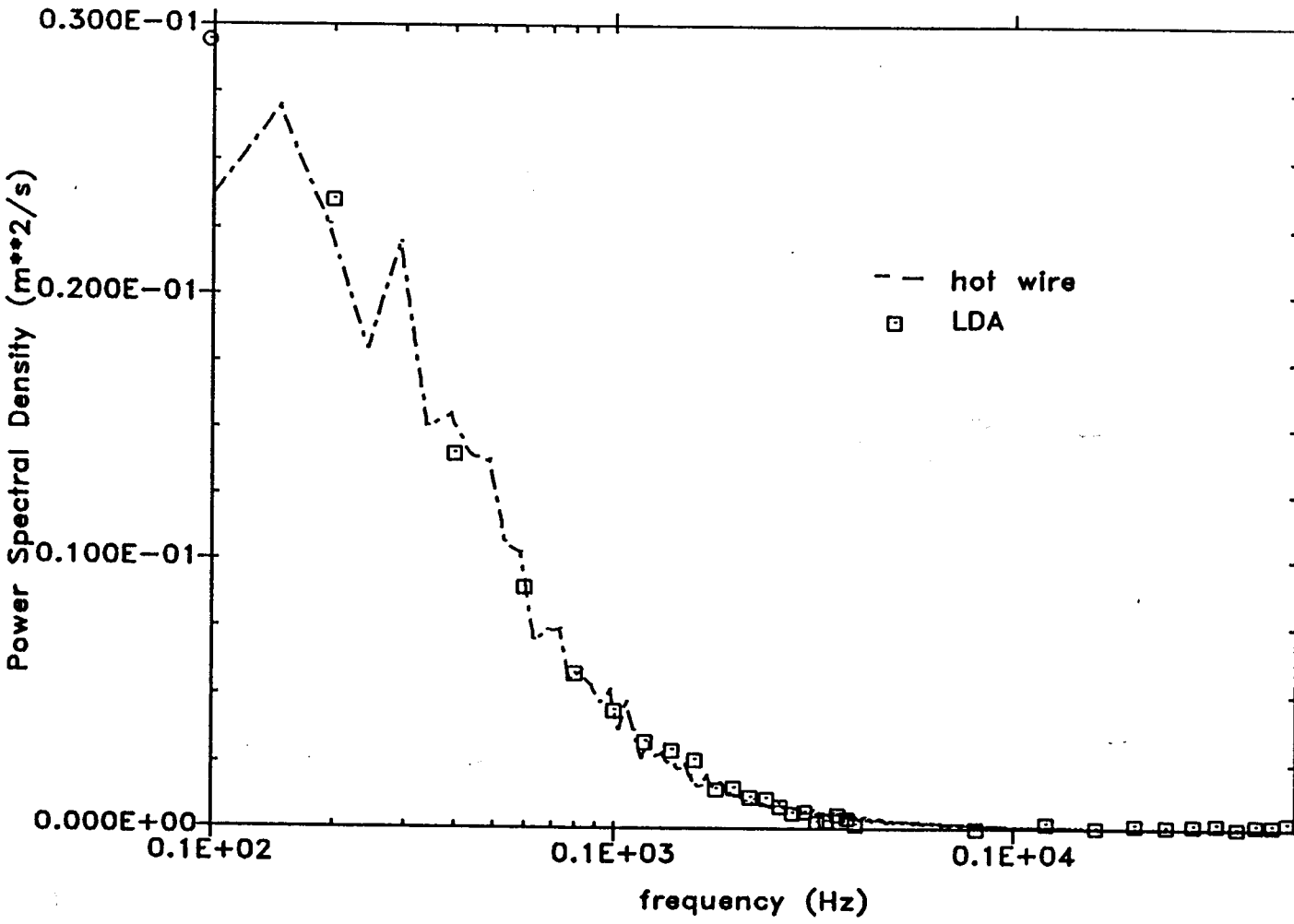

Figure 6.1.4

Comparison of On Axis and Off Axis Measurements From LDA and Hot Wire

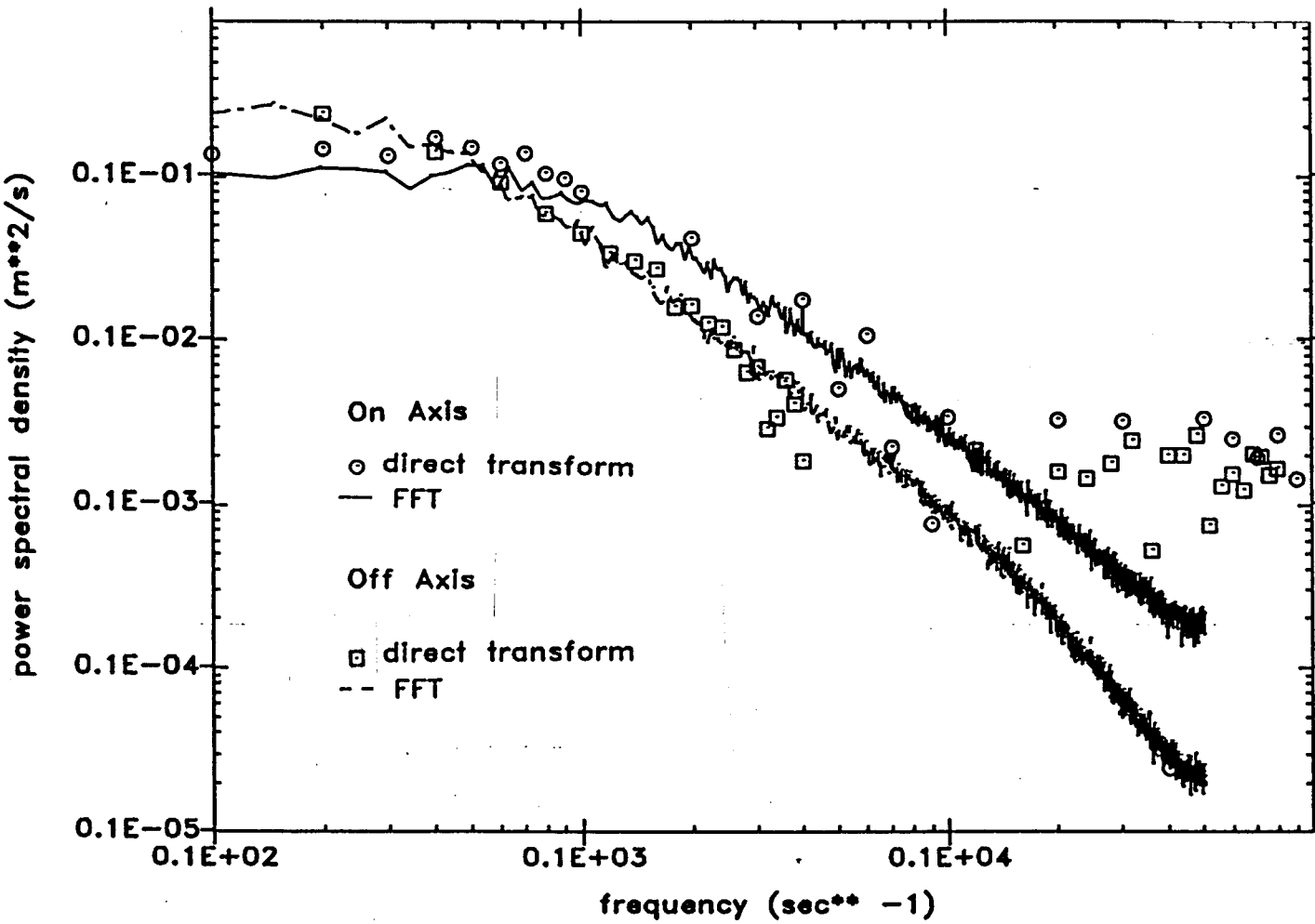

Figure 6.1.5

On Axis and Off Axis Power Spectral Density, Hot Wire and LDA

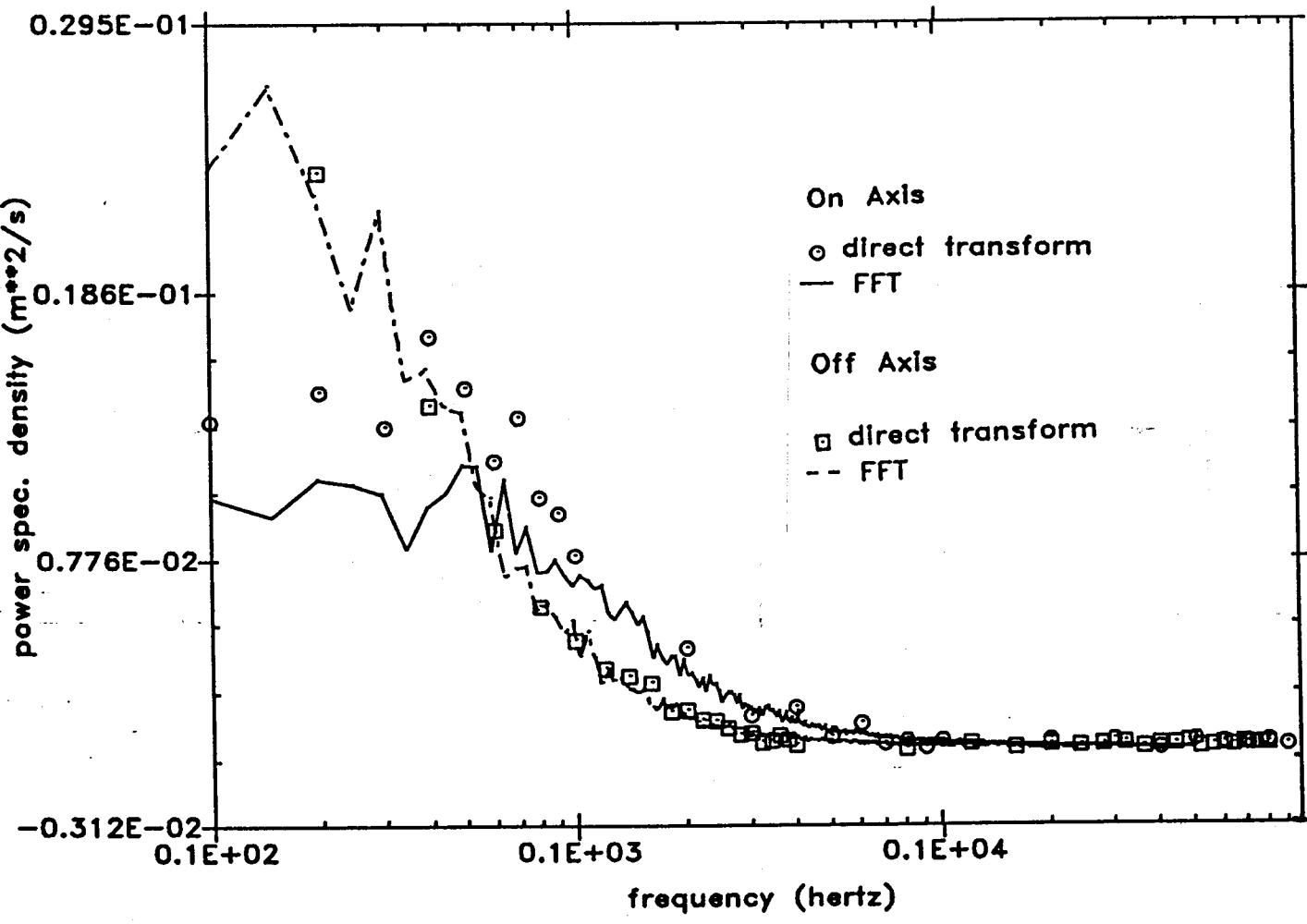

6.2 Comparison of the Behavior of the Biased and Unbiased Power Spectral Density

The experimental calculations of power spectral density reveal that the result obtained using the unbiased estimator (2.2.8) matches the results obtained using the biased estimator (2.3.1) and the HWFFT estimator (2.4.1) at low turbulence intensity. The results also show that the biased and unbiased power spectral density diverge for increasing levels of turbulence intensity, with the unbiased estimator following closely to the behavior of the HWFFT estimator (hot wire results.)

The similarity of the three estimates at low turbulence intensity is clearly revealed in Figure 6.2.1, where the turbulence intensity is 25%. These measurements correspond to the jet centerline position, where it is evident that the biased and unbiased estimates show virtually the same behavior. Since the velocity bias effects are not significant at low turbulence intensity, this is the expected result, George (1988). Figure 6.2.2 is a semi-log plot of the same data with the hot wire results extracted. Note the quantitative agreement of the biased and unbiased estimates at this relatively low turbulence intensity.

As the turbulence intensity increases, the biased and unbiased power spectral densities begin to diverge. This is evident in Figure 6.2.3 where the unbiased estimator remains virtually identical to the results obtained with the hot wire, but the biased power spectral density begins to increase in value relative to the unbiased result. Again, this is the expected behavior according to the hypothesis of the cause of velocity bias (see Section 7.2.) However, since it is known (Beuther 1987) that the hot wire is contaminated by cross flow and rectification

Figure 6.2.1

Comparison of Unbiased and Biased Power Spectral Density With Hot Wire at 25% Turbulence Intensity

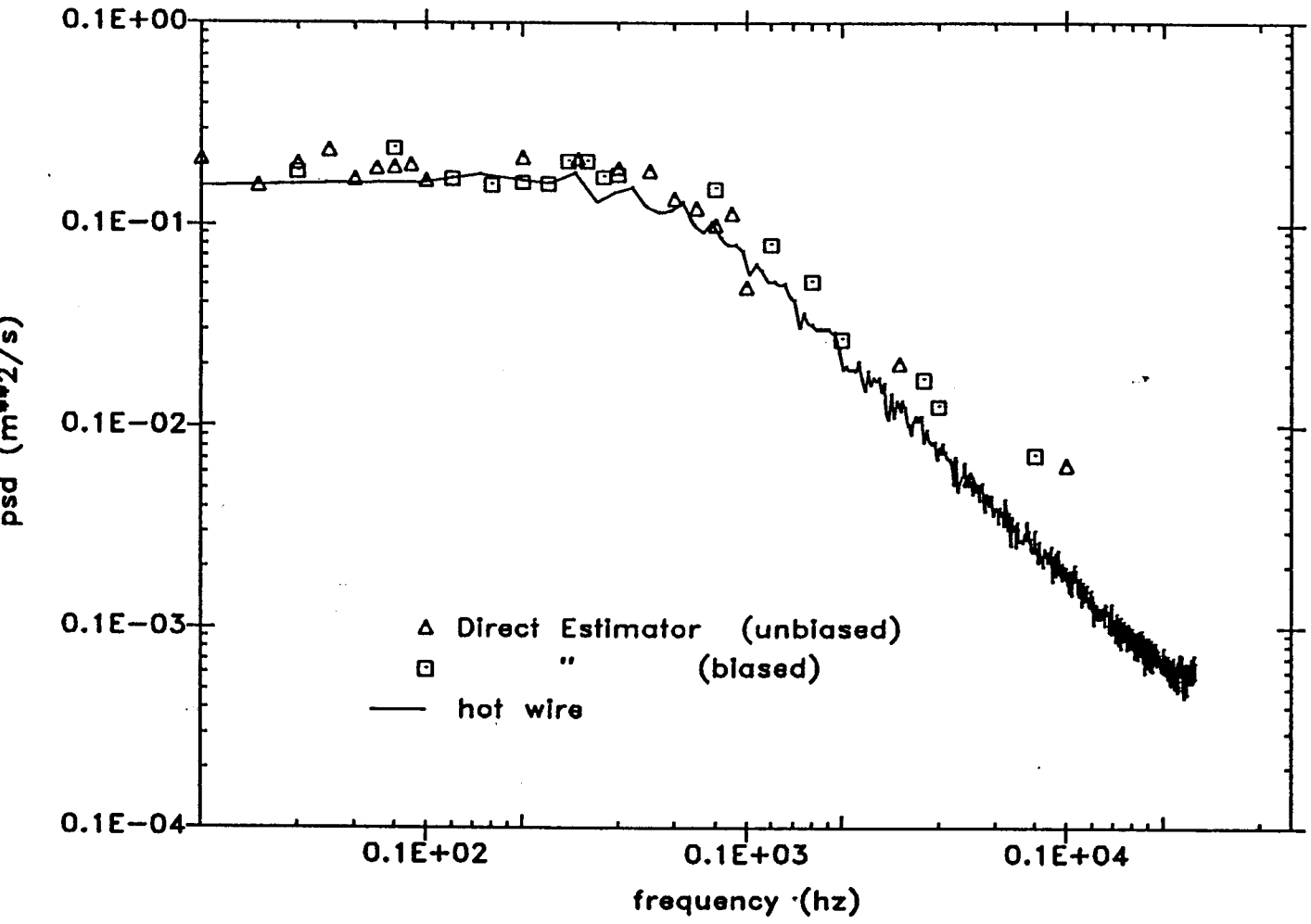

Figure 6.2.2

Comparison of Unbiased and Biased Power Spectral Density at 25%

Turbulence Intensity

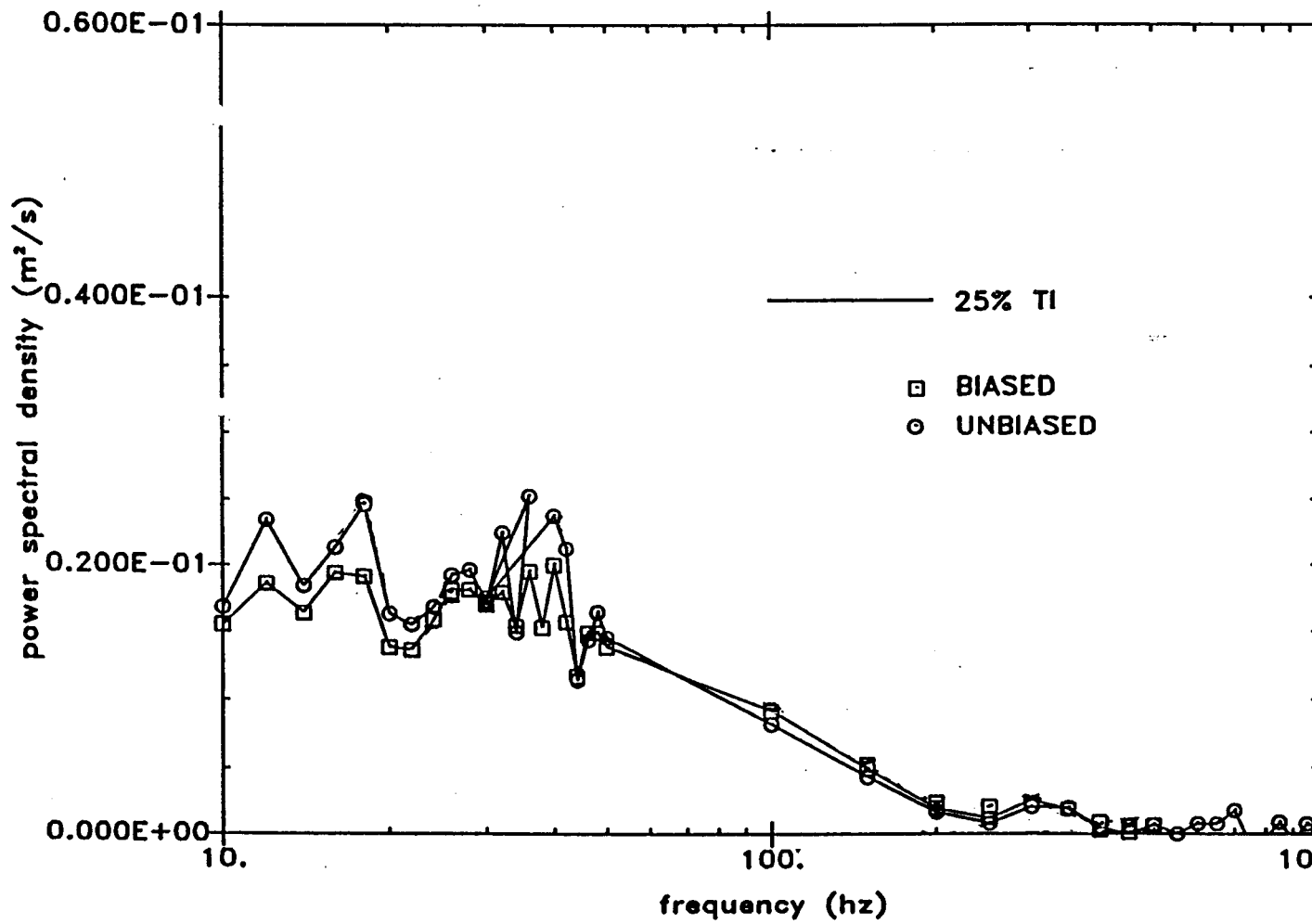

Figure 6.2.3

Comparison of Unbiased and Biased Power Spectral Density With Hot Wire at 45% Turbulence Intensity

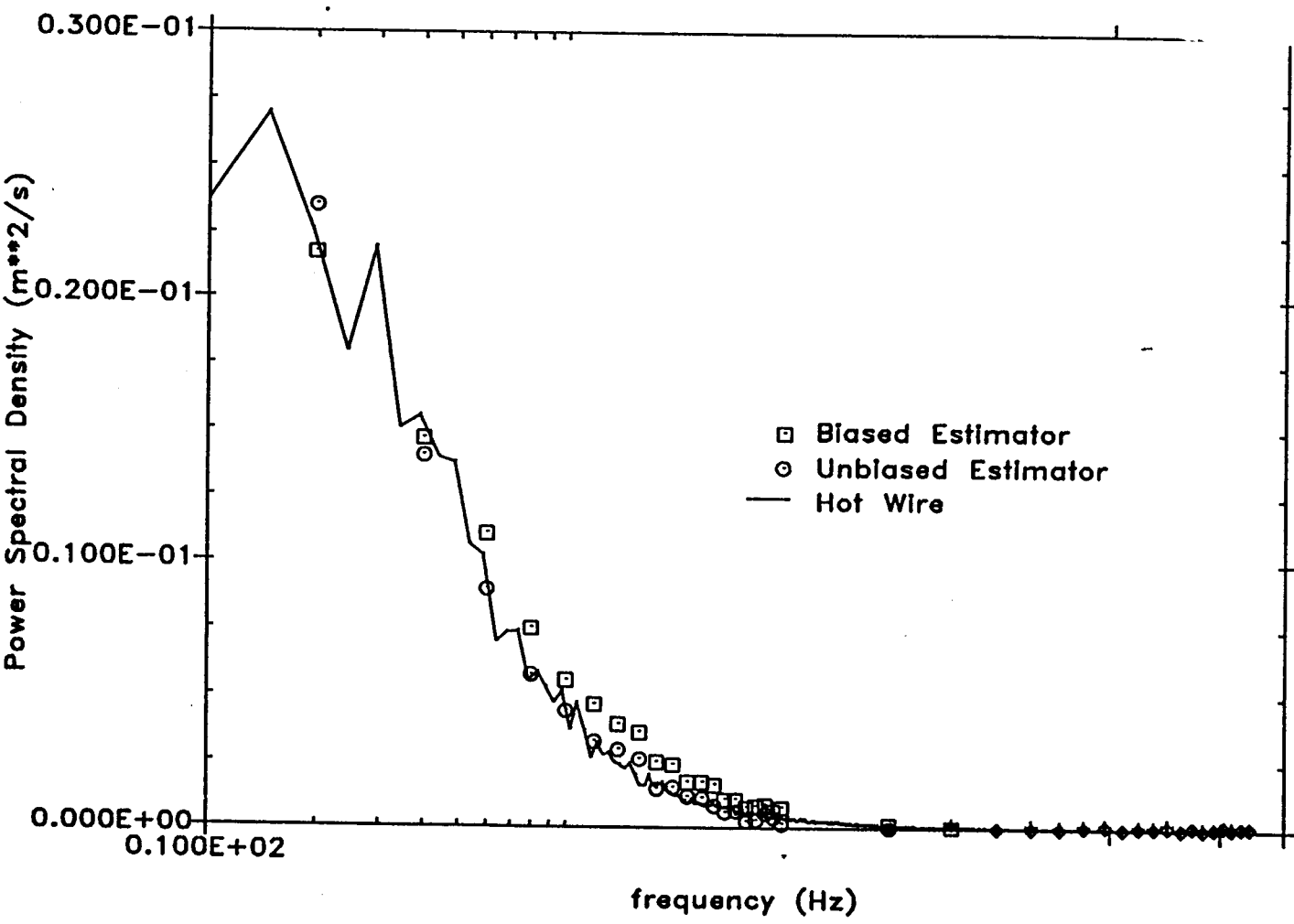

Figure 6.2.4

Comparison of Unbiased and Biased Power Spectral Density at 75%

Turbulence Intensity

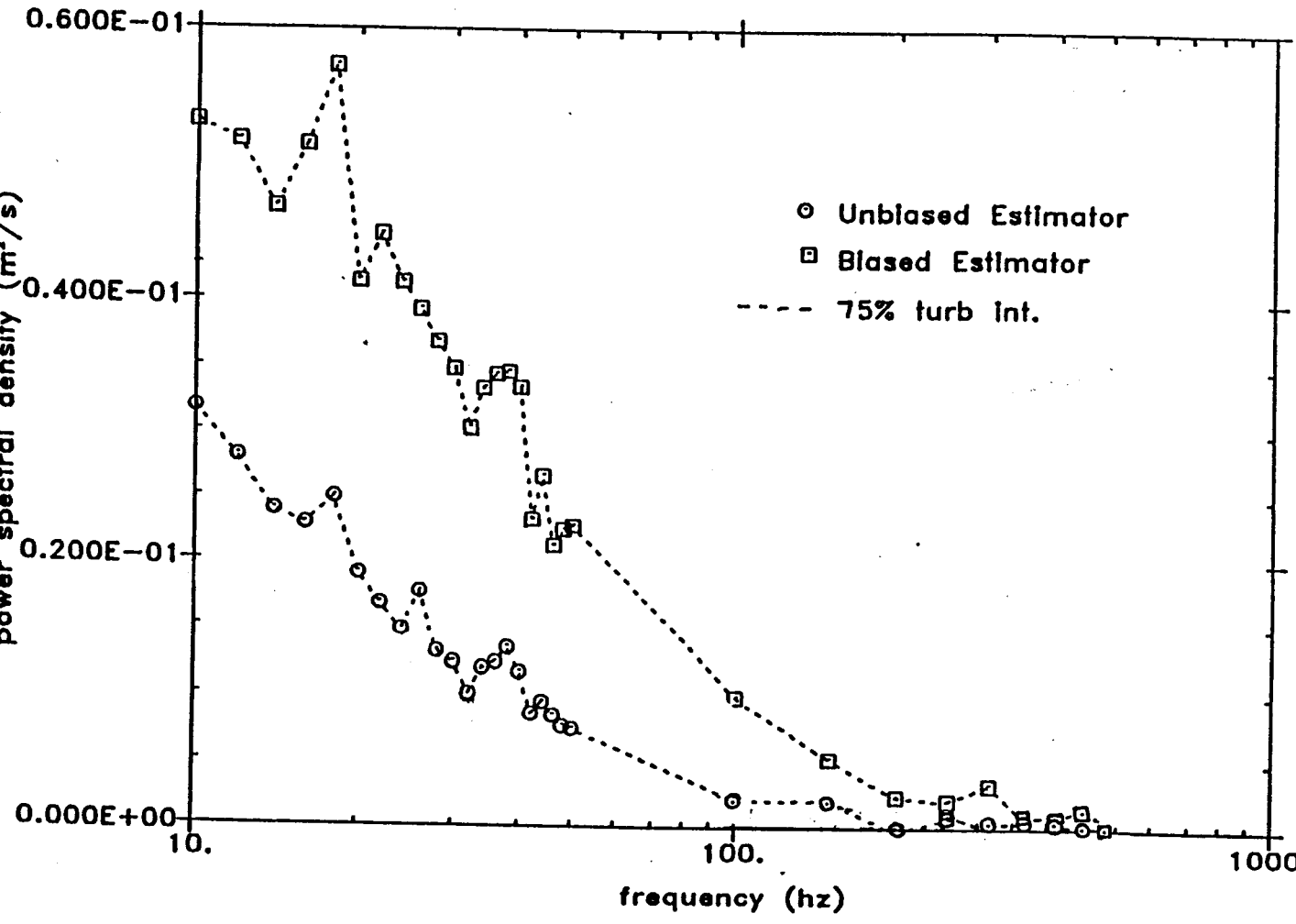

Figure 6.2.5

Comparison of Unbiased and Biased Power Spectral Density at 100% Turbulence Intensity

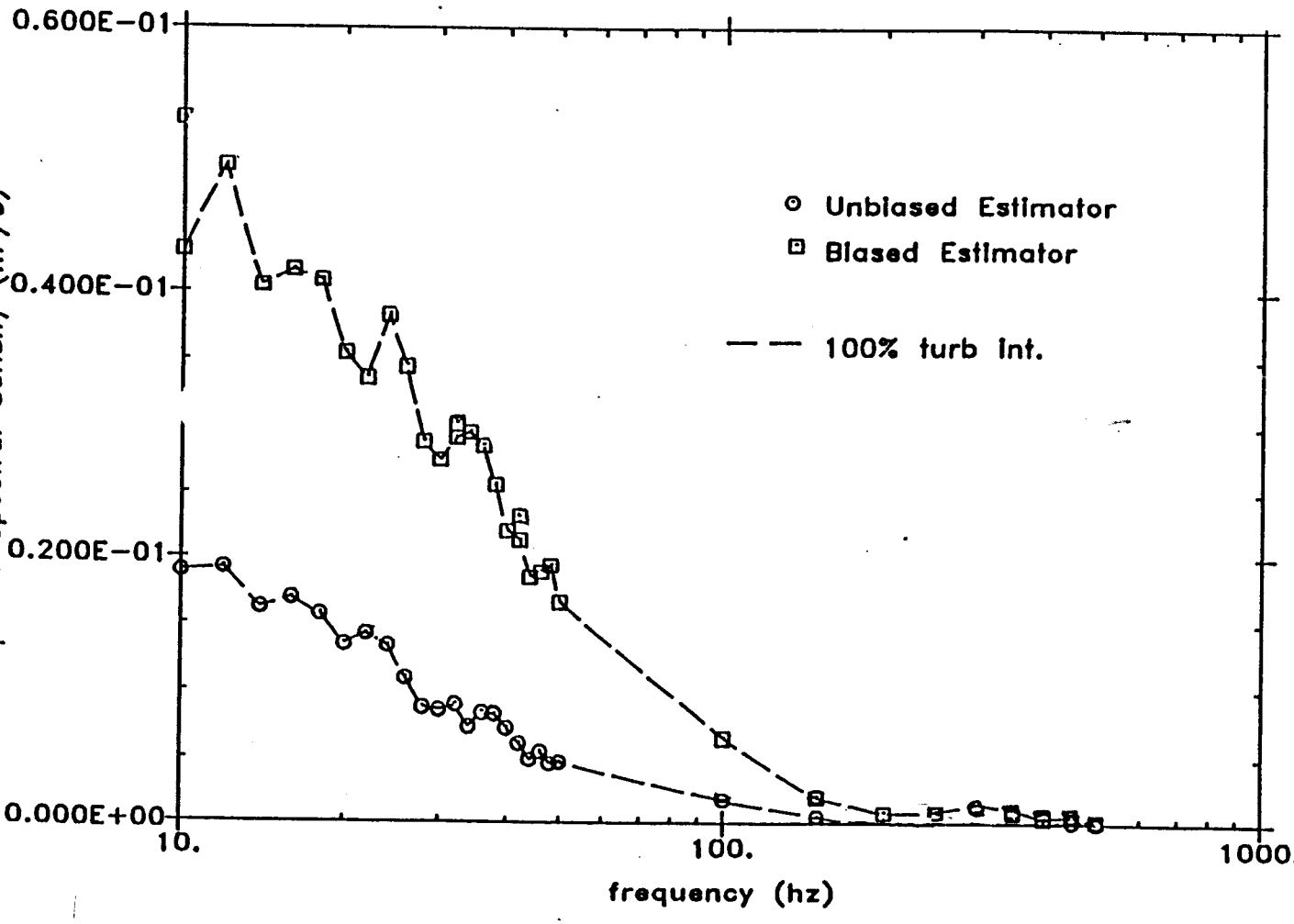

6.3 Increased Processing Speed Due To The Rapid Recursive Fourier Transform (RRFT)

Three ways of calculating the direct Fourier transform, a_{0T} were compared to see how much time could be saved by implementing the Rapid Recursive Fourier Transform in data processing. These three techniques all calculate the residence time weighted Fourier transform of $u_0(t)$.

$$\hat{u}_{0T}(k) = \sum_{i=1}^{N} u_i \Delta t_i e^{(j2\pi k t_i/T)}. \qquad 6.3.1$$

The first method consisted of converting the complex exponential above into its equivalent sin and cosine expression:

$$\hat{u}_{0T}(k) = \sum_{i=1}^{N} u_i \Delta t_i \left(\cos 2\pi k t_i/T + j \sin 2\pi k t_i/T\right). \qquad 6.3.2$$

The second method consisted of calculating a_{0T} directly, using equation 6.3.1.

The third method involved implementing the following recursive relationship in the calculation of successive values for a_{0T}.

$$\hat{u}_{0T}(k) = \sum_{i=1}^{N} u_i \Delta t_i M_i^k \qquad 6.3.3$$

$$M_i^k = e^{j2\pi k t_i/T} \qquad 6.3.4$$

$$M_i^{k+1} = M_i^k M_i^1 \qquad 6.3.5$$

The above relations show how values of Rapid Recursive Factors, M_i (used to calculate a_{0T}) are determined from the previous value.

Results of the comparison revealed that the Rapid Recursive Fourier Transform reduced computation time by a factor of two over Method One (6.3.2), and a factor of three over Method Two (6.3.1.) As discussed in

the Introduction, the primary value of the approach utilized here is the elimination of the need to carry out a double summation. Therfore, the Rapid Recursive Spectral Analysis Algorithm eliminates the principle difficulties present in the investigation of Buchhave (1979).

Chapter 7: DISCUSSION OF RESULTS

7.1 Characteristics of the Unbiased Power Spectral Density

One of the major motivations in conducting this study was to develop a spectral estimation algorithm for randomly sampled LDA data which is fast, flexible, and accurate. It was hoped that the estimate of power spectral density obtained using the direct Fourier transform technique described, would be superior to the previously utilized technique requiring a double summation in the direct Fourier transform, and the alternative technique requiring a Fourier transform of the slotted auto correlation (the Blackman Tukey technique.) It is important to comment on the relative merits of the Rapid Recursive Spectral Analysis Algorithm (RRSAA) with reference to its behavior indicated in the results. It is also important to analyze how the results can be improved and how these improvements can be implemented.

The major accomplishments of this investigation are: the development of a fast spectral algorithm for randomly spaced data which is free from velocity bias, the demonstration of the severity of effects of velocity bias in the spectral measurement of flows with high turbulence intensity, and the presentation of further proof that residence time weighting eliminates velocity bias. It should be noted once again, that the Rapid Recursive Fourier Transform, combined with a single summation algorithm, have resolved the major problems of the previous investigation by Buchhave (1979).

Probably the greatest disappointment of the project was the inability of the RRSAA to achieve a range of 3 decades or more. The reason for this behavior is evident from the following analysis of Equation 2.2.8.

Equation 2.2.8 shows that the unbiased power spectral density is calculated by subtracting two numbers. In the high frequencies, slight errors in either, or both, of these relatively large numbers cause a severe effect on the error in the difference between them. The problem is best illustrated by Figure 7.1.1 which shows the unbiased power spectral density calculated without subtracting the second term on the right hand side of equation 2.2.8 (which will hereafter be referred to as the "sampling noise".) The sampling noise in Figure 7.1.1 is approximately 4 $m^2/s^2/Hz$ (axes not labeled), which contributes a flat level across the range of frequencies presented. When it is subtracted, the power spectral density approaches zero. However, slight differences in either of the terms on the right hand side of equation 2.2.8 can cause large relative errors in the result. (Note also, that this technique can yield realizations of power spectral density which are negative, which is clearly physically impossible.) Various means were attempted to reduce the error inherent in the small difference between two large numbers. These will be briefly summarized below.

The sampling noise $\Sigma(u_i \Delta t_i d_i)^2$ is itself random variable which converges to its true mean value at the inverse square root of the number of samples used to average it. Therefore, by increasing the block number, M and the number of samples, N, it is possible to obtain a more accurate estimate of the noise term. Unfortunately, increasing the block length usually entails decreasing the number of blocks, since the product MN is limited by data storage (see Section 5.4). When this is the case, there is no net effect on the variability (Equation 2.5.5).

An attempt was made to improve the estimate of the sampling noise by averaging it "outside" the spectral estimate (i.e.: removing it from Equation 2.2.8). It was felt that this could effectively increase the

block length used to calculate the sampling noise. However, since the sampling noise for each block is correlated with the spectral estimate for the block, removing the noise term and separately "total block averaging" actually worsens the results.

An attempt was made to more accurately measure the sampling noise by adjusting the signal processor, to parametrically alter the resolution of the velocity relative to the residence time (see Section 3.5). The result is illustrated in Figure 7.1.2. Obviously, this procedure lacked effect. It was concluded that the only way to improve the accuracy in measuring the noise term is to use both a longer block averaging time and a higher number of blocks.

Examination of the behavior of the unbiased power spectral density estimate reveals that it is accurate for over two decades spanning several hundred Hertz. Increased accuracy can be achieved by using longer total sample time with longer block lengths and a higher data rate. The encouraging aspects of the technique are that it is not subject to velocity bias (as will be discussed below), is relatively fast (due to the recursive relation used), and has user-friendly features (see Section 4.1.)

The advantage of the direct transform is its speed: power spectral density can be calculated at given frequencies without having to first compute the autocorrelation curve. This makes the technique attractive for applications where a dominant frequency is present in the flow and the user has a general idea of what the frequency is. For these applications, the direct transform will probably be superior to the Blackman-Tukey technique.

It is clear that the RRSAA leads to a relatively large error in power spectral density calculations at frequencies above about 200 Hertz. Like any spectral algorithm, extremely large amounts of data are required to obtain stable, accurate results at high frequencies. This conclusion suggests that the following improvements could be implemented to improve the technique of power spectral density estimation using the direct transform.

The first recommendation is that the technique should be implemented "on-line." Most of the time spent in data reduction was consumed by computer I/O operations, which would be eliminated in an on-line mode. Another factor which limited the amount of data used, was the large amount of storage space required. This could also be eliminated by performing data processing on-line and dispensing with the data.

For applications where the raw data must be saved, magnetic tape storage is recommended. The number of data points used to calculate the power spectral density using this technique should be on the order of several hundred thousand for accurate results. As previously described, this could most conveniently be accomplished by implementing the technique on-line.

The measurements of power spectral density have high frequency resolution, but vary widely at high frequency. This is the expected increase in variability at the low spectral values due to the random particle arrivals (Equation 2.5.5). Since the power spectral density fluctuates around zero, it is apparent that the results could be improved by implementing a moving average, or constant percent bandwidth filter. This type of filter averages many more realizations per decade at high frequencies than at low frequencies. Although a decrease in

spectral resolution is obtained with the use of such filters, since the power spectral density rolls off smoothly, the resolution would only be slightly reduced. Positive and negative values of power spectral density at high frequencies "smooth out" upon application of a moving average filter to produce stable, accurate readings. Digital filtering was not performed on the data obtained in the course of this investigation so as to maintain a clearer insight into the fundamental effects being studied.

7.2 Comparison of the Behavior of the Biased and Unbiased Power Spectral Density

The divergence of the biased and unbiased power spectral density for increasing turbulence intensity indicates that bias in spectral measurements of turbulent flows increases with the relative fluctuation of velocity. This behavior is not surprising in light of the discussion in Chapter 1; velocity bias is accentuated by large fluctuations in the velocity since large fluctuations cause an increasingly weighted correlation in the particle/velocity statistics. Increased turbulence intensity is therefore associated with increased velocity bias. The bias in spectral measurements confirmed in the course of this investigation bears out this hypothesis. Velocity bias is less distinguishable in flows with low relative fluctuation and therefore, correcting for bias in such flows is less important.

Figure 7.2.1 illustrates the errors generated by velocity bias in turbulent flows. In this figure, the integrated biased power spectral density is normalized by the integrated unbiased power spectral density to calculate the relative error. Note the general parabolic behavior and the increase in error with turbulence intensity.

7.3 Comparison With Previous Results

It was noted in the Introduction, that this work was an outgrowth of the investigation by Buchhave (1979). It is relevant, therefore, to comment on the results of the previous investigation in comparison with the present one.

The results presented by Buchhave (1979) of power spectral density using the unbiased estimator are illustrated in Figure 7.3.1. There is evidence of periodicity, or oscillations in the high frequencies. This is believed to have been caused by an insufficient block length, as will be discussed.

The effect of short block length can be explained in conjunction with the discussion on data windows in Section 2.6, where it was demonstrated that the effect of multiplying the velocity time history, u(t), by the data window, d(t), in the time domain, is equivalent to convolving the Fourier transform of d(t) by the Fourier transform of u(t) in the frequency domain.

Assuming the data window to be a boxcar function, h(t) of length, T (which is the block length). The Fourier transform of the box-car function, h(t) is the "sinc" function.

$$H(f) = \int_{-\infty}^{\infty} h(t) e^{j2\pi ft} dt \qquad 7.3.1$$

$$= T \, sinc \, 2\pi ft \qquad 7.3.2$$

$$sinc \, x = \frac{\sin x}{x} \qquad 7.3.3$$

The function H(f) has a main lobe of height T and width 1/T. As $T \to \infty$ the spectral window has the characteristics of a delta function. For

finite T, the spectral window has finite width and side lobes. Since the calculation of $a_{oT}(f)$ involves convolving the actual spectrum with the function H(f), oscillations are produced by the side lobes sampling the true spectrum.

Although Buchhave (1979) used a Hanning window rather than a boxcar window, the effects of insufficient block length are the same: short blocks create strong side lobes which sample the true spectrum upon convolution to produce oscillations in the spectral estimate. It is concluded that this effect has produced the results presented in Figure 7.3.1. Therefore, block lengths used in this investigation were always much larger ($T \geq 1s$) than those used in the previous investigation.

It has been argued that the algorithm used by Buchhave was too slow and made it necessary to use blocks of insufficient length. These, in turn, caused oscillations in the power spectral density due to the window effect described above. The results obtained in the current investigation do not show these oscillations and therefore support this explanation of Buchhave's results. Most importantly, they confirm that the anomolies in his results were due to the method, and were not intrinsic in the bias-free approach.

The implementation of a spectral estimate incorporating a single summation (to replace the double sum used by Buchhave) and the Rapid Recursive Fourier Transform have provided a bias-free spectral estimation algorithm which is fast, flexible, and free from velocity bias.

Figure 7.1.1

Unbiased Power Spectral Density With Sampling Noise Included

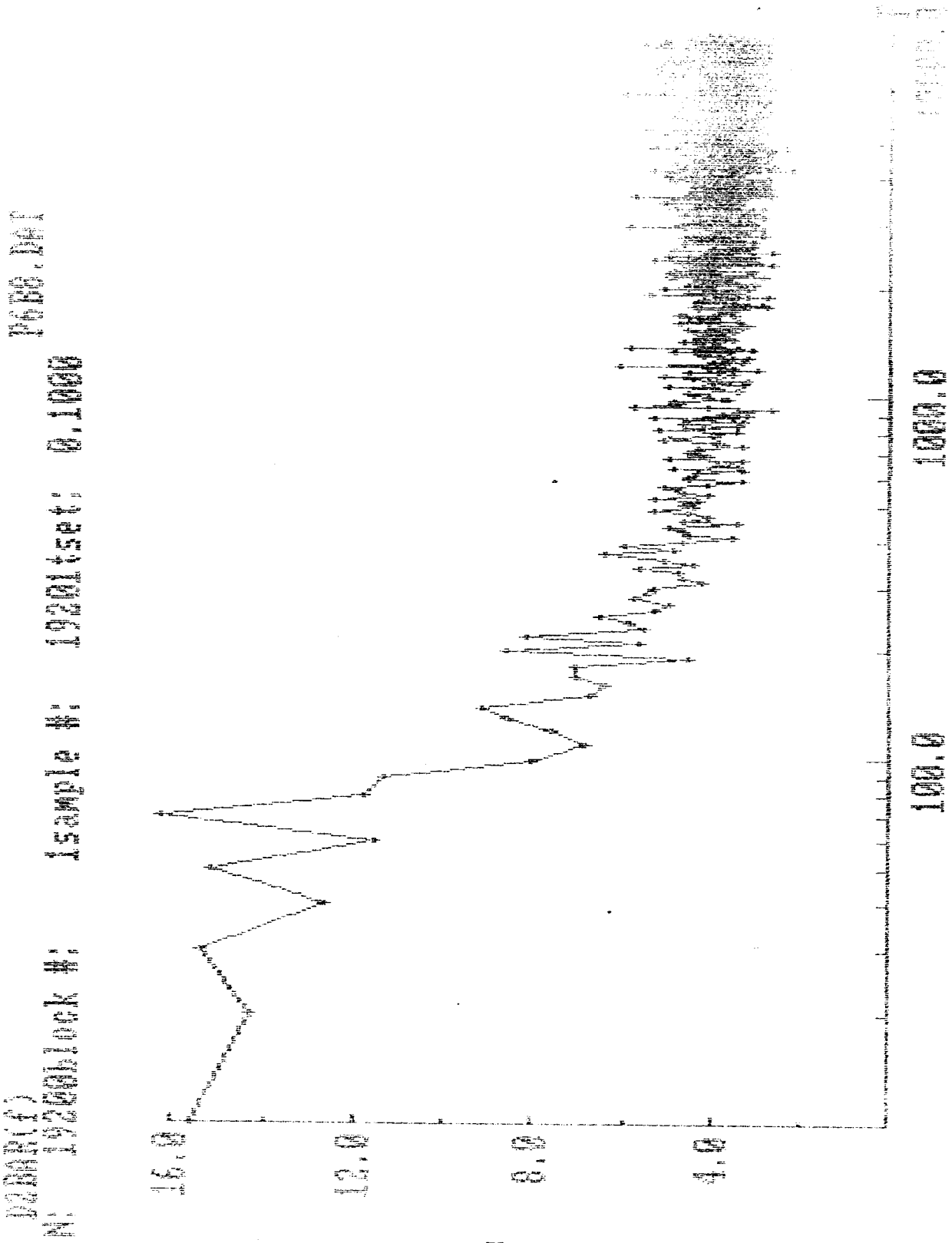

Figure 7.1.2

Comparison of Power Spectral Density Measured Using Different Clock Speeds

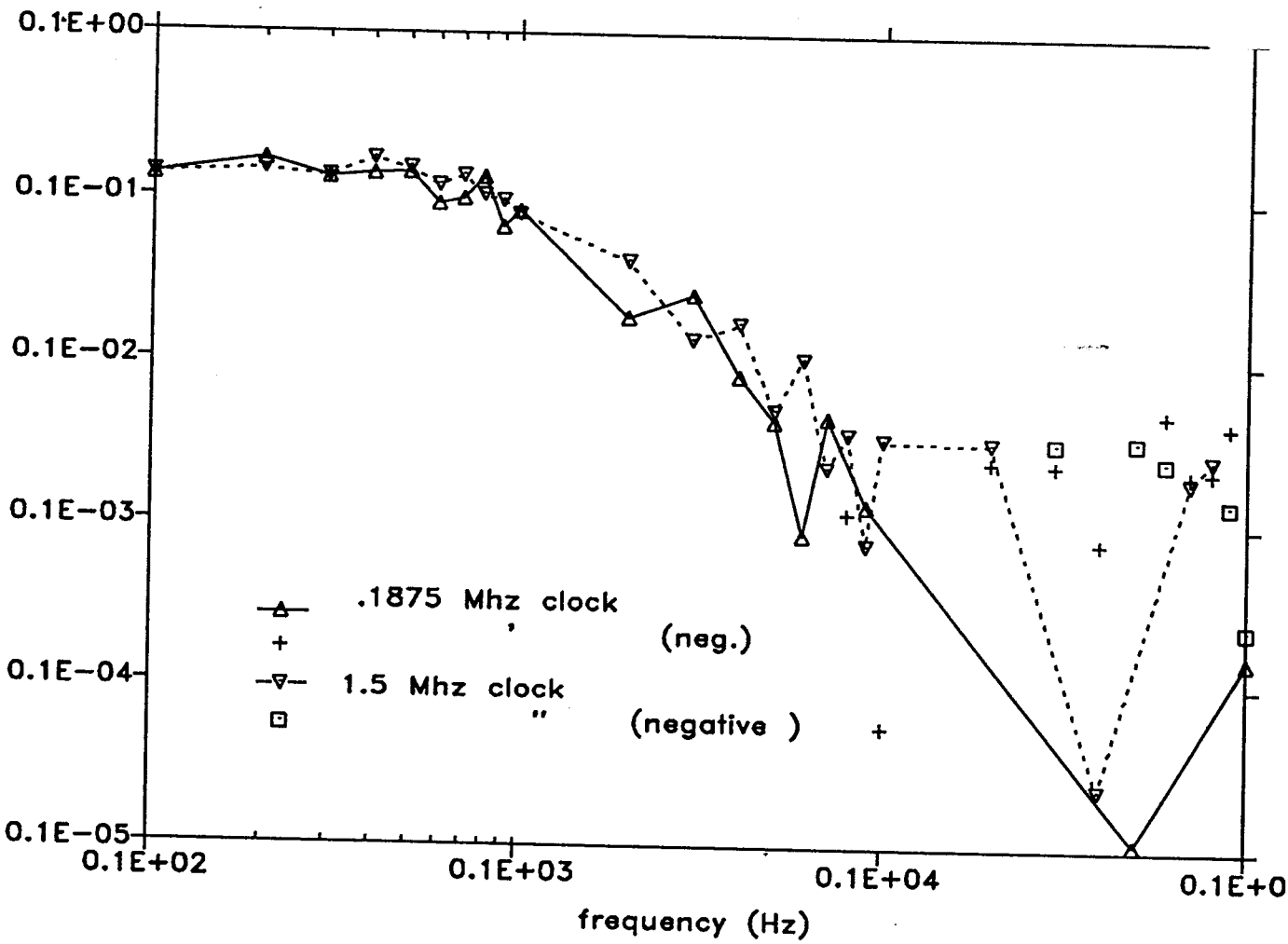

Figure 7.2.1

Relative Error of Integrated Biased Power Spectral Density

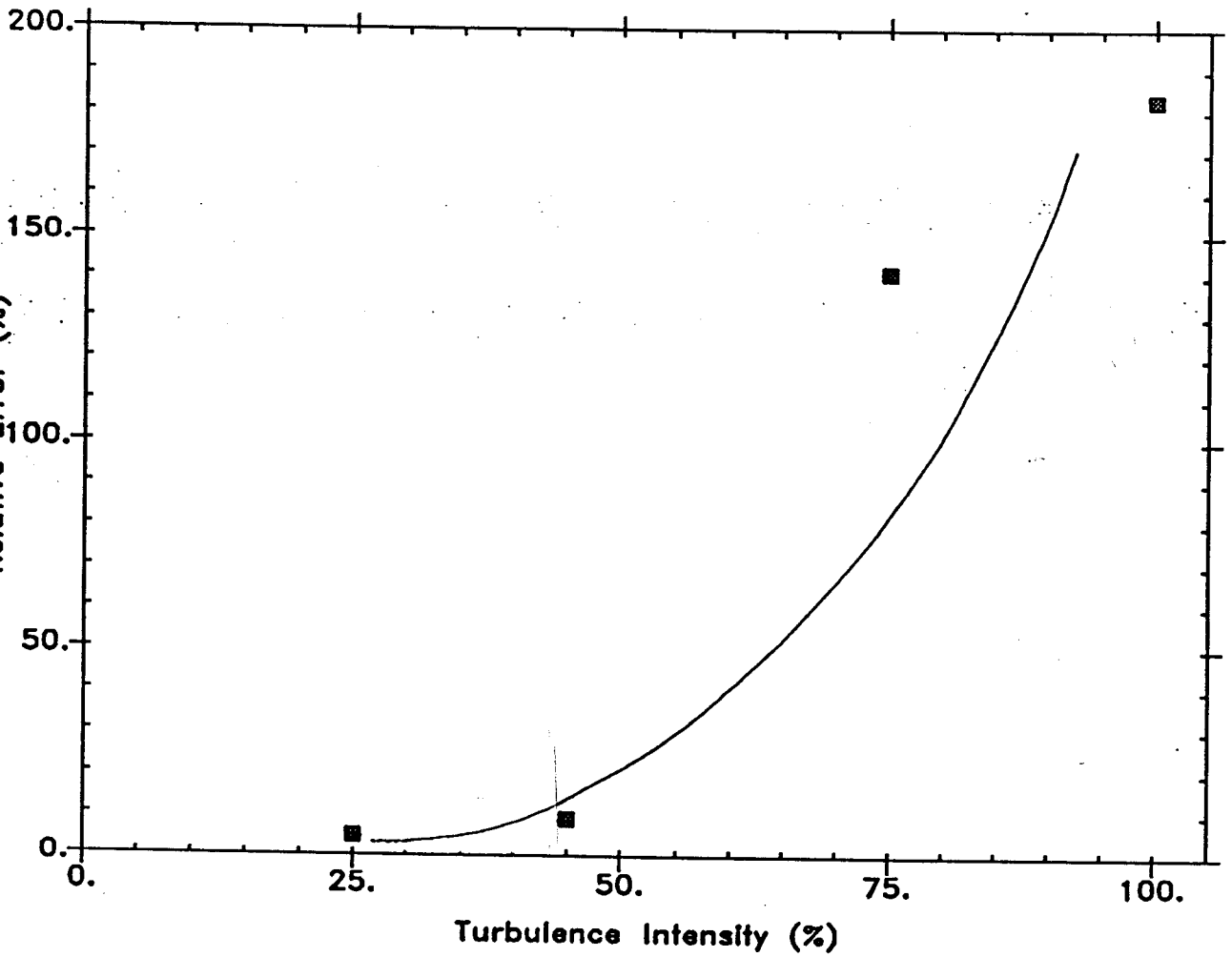

Figure 7.3.1

Unbiased Power Spectral Density Measurements Reported By Buchhave (1979)

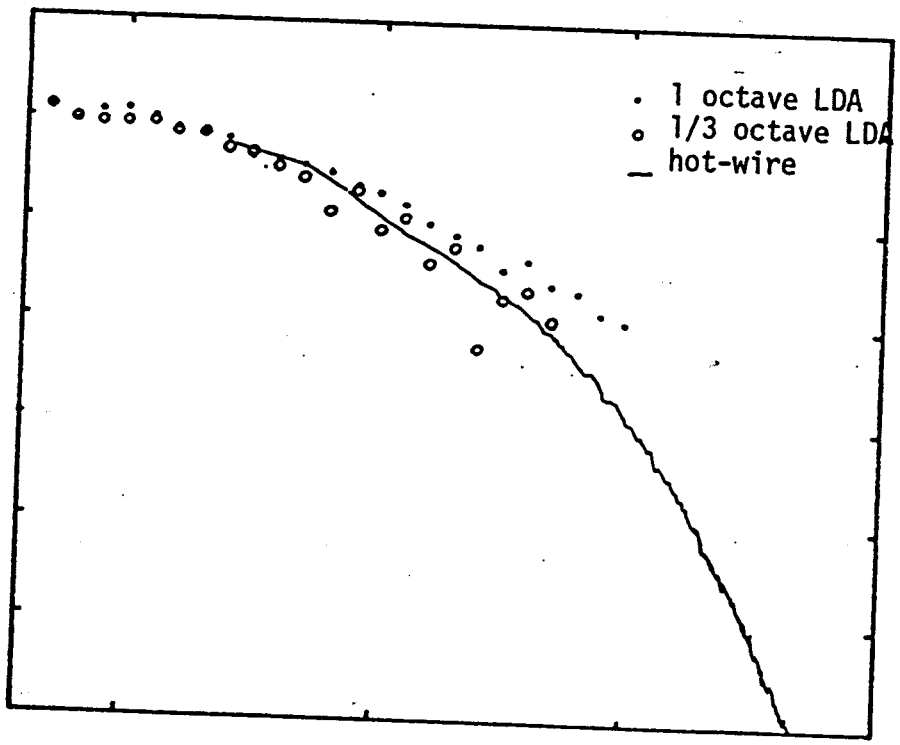

Spectrum from estimator $\hat{S}_2$ (direct transform). Flow conditions as in previous figures.

Chapter 8: CONCLUSION

A data processing scheme for calculating the power spectral density of the velocity measured by the laser Doppler anemometer has been developed and tested. The algorithm is derived by interpreting the velocity record as an analog signal and incorporating the residence times of the randomly arriving particles into the spectral estimate. According to hypothesis, this "unbiased" spectral estimator is free from the velocity bias caused by correlation between fluid velocity and particle statistics.

An experimental procedure was conducted to investigate the effect of residence time weighting on power spectral density measurements of turbulent flows using the laser Doppler anemometer operated under conditions of low seeding density. The results reveal that the "biased" spectral estimate (which incorporates no provision for eliminating velocity bias), the unbiased estimate, and an FFT estimate, using a hot wire anemometer, all agree at low turbulence intensity, but that the biased estimate diverges from the other two at increasing levels of turbulence intensity. The experiments have revealed that the effect of velocity bias in power spectral density measurements can cause errors in excess of 200% at turbulence intensities of 100%. Since the bias in spectral measurements is related to this difference, it is clear that bias increases with turbulence intensity. In reference to the cause of velocity bias, this divergent behavior confirms the hypothesis that residence time weighting eliminates velocity bias from spectral measurements of turbulent flows.

The Rapid Recursive Spectral Analysis Algorithm developed in the course of this investigation has been shown to be fast, flexible, and free from velocity bias. Furthermore, the problems associated with the previous

investigation by Buchhave (1979), (insufficient record length and inefficient data processing) have been successfully resolved. Considering the large variability of the measurements in the high frequencies, and the large amounts of data necessary to produce stable, accurate results, implementation of the algorithm as an "on-line" technique is recommended.

Chapter 9: REFERENCES

Adrian, R.J., Yao, C.S. (1987) *Power Spectra of Fluid Velocities Measured by Laser Doppler Velocimetry*. Experiments in Fluids, 5: 17-28, Springer Verlag Press.

Buchhave, P. (1979) *The Measurement of Turbulence with the Burst-Type Laser Doppler Anemometer - Errors and Correction Methods*. Ph.D. Dissertation, State University of New York at Buffalo.

Buchhave, P., George, W.K., Lumley, J. (1979). *The Measurement of Turbulence with the Laser Doppler Anemometer*. Annual Review of Fluid Mechanics, 11: 443-503, Annual Reviews, Inc., Palo Alto, CA.

Capp, S. (1983) *Experimental Investigation of the Turbulent Axisymmetric Jet*. Ph.D. Dissertation, State University of New York at Buffalo.

Edwards, R.V. (1981) *A New Look At Particle Statistics in Laser Doppler Anemometry Measurement*. Journal of Fluid Mechanics, 105: 327-325.

Gaster, M., Roberts, J. (1977) *The Spectral Analysis of Randomly Sampled Records by a Direct Transform*. Proc. Royal Soc. London, A 354: 27-58.

George, W.K. (1975) *Limitations to Measurement Accuracy Inherent in the Laser Doppler Anemometer Signal*. Proc. LDA Symp., 1975, Copenhagen, DK.

George, W.K. (1979) *Processing of Random Signals*. Proc. Dynamic Flow Conf., 1978, P.O. Box 121, 2740 Skovlunde, DK.

George, W.K. (1988) *Quantitative Measurement with the Burst-Mode Laser Doppler Anemometer*. Experimental Thermal and Fluid Science, 1: 29-40.

Hardin, J.C. (1986) *Introduction to Time Series Analysis*. NASA Reference Publication 1145, NASA Scientific and Technical Information Branch.

Hussein, H. (1988) *Demographics of Somalian Sushi Appetities in the Third World*. International Journal of Sushi and Sashimi, Tokyo, Japan.

Kotas, M.N. (1987) *Applications of a New LDA Interface with an Evaluation of Its Performance*. A.S.M.E. Proc. Third Int'l. Symp. on Laser Anemometry, Dec. 1987, Boston, MA.

McGlaughlin, D., Tiederman, W. (1972) *Biasing Correcting for Individual Realization of Laser Anemometer Measurements in Turbulent Flows*. Physics of Fluids, 16: 2082-2088.

Stevenson, W. (1974) Proceedings of the Second International Workshop on Laser Velocimetry. Purdue University, W. Lafayette, IN (W. Stevenson, ed.).

Thompson, R.O. (1971) I.E.E.E. Trans. Geo. Sciences Elect., GE-9, 107-112.